JAERI-M
87-093

MAIN PHYSICS FEATURES DRIVING DESIGN CONCEPT AND PHYSICS DESIGN CONSTRAINTS -CONCEPTUAL DESIGN STUDY OF FY86 FER-

July 1987

Noboru FUJISAWA, Masayoshi SUGIHARA, Shin YAMAMOTO
Tadanori MIZOGUCHI[*1], Shigehisa HITOKI[*2], Mitsushi ABE[*3]
Noriaki UEDA[*4], Takashi OKAZAKI[*3], Kunihiko OKANO[*5]
Masao KASAI[*4], Kichiro SHINYA[*5] and Akiyoshi HATAYAMA[*5]

日 本 原 子 力 研 究 所
Japan Atomic Energy Research Institute

JAERI-Mレポートは，日本原子力研究所が不定期に公刊している研究報告書です。
入手の問合わせは，日本原子力研究所技術情報部情報資料課（〒319-11 茨城県那珂郡東海村）あて，お申しこしください。なお，このほかに財団法人原子力弘済会資料センター（〒319-11 茨城県那珂郡東海村日本原子力研究所内）で複写による実費領布をおこなっております。

JAERI-M reports are issued irregularly.
Inquiries about availability of the reports should be addressed to Information Division Department of Technical Information, Japan Atomic Energy Research Institute, Tokaimura, Naka-gun, Ibaraki-ken 319-11, Japan.

編集兼発行　日本原子力研究所
印　　刷　日青工業株式会社

JAERI-M 87-093

Main Physics Features Driving Design Concept and Physics Design Constraints -Conceptual Design Study of FY86 FER-

Noboru FUJISAWA, Masayoshi SUGIHARA, Shin YAMAMOTO
Tadanori MIZOGUCHI[*1], Shigehisa HITOKI[*2], Mitsushi ABE[*3]
Noriaki UEDA[*4], Takashi OKAZAKI[*3], Kunihiko OKANO[*5]
Masao KASAI[*4], Kichiro SHINYA[*5] and Akiyoshi HATAYAMA[*5]

Department of Large Tokamak Research
Naka Fusion Research Establishment
Japan Atomic Energy Research Institute
Naka-machi, Naka-gun, Ibaraki-ken

(Received June 8, 1987)

Major physics design philosophies are described, which are essential bases for a plasma design and may have significant impacts on a reactor design concept. Those design philosophies are classified into two groups, physics design drivers and physics design constraints. The design drivers are featured by the fact that a designer is free to choose and the choice may be guided by his opinion, such as ignition, a pulse length, an operation scenario, etc.. The design constraints may follow a physical law, such as plasma confinement, β-limit, density limit, and so on.

Keywords: Design Driver, Design Constraint, FER, INTOR

---

*1 On leave from Hitachi, Ltd.
*2 On leave from Mitsubishi Electric Co., to which he returned back.
*3 Hitachi, Ltd.
*4 Mitsubishi Atomic Power Industries
*5 Toshiba Corporation

JEARI-M 87-093

設計概念を決める主要物理特性と物理設計条件
—次期大型装置設計（FY86 FER）—

日本原子力研究所那珂研究所臨界プラズマ研究部
藤沢　登・杉原　正芳・山本　新・溝口　忠憲[*1]
一木　繁久[*2]・阿部　充志[*3]・上田　憲照[*4]・岡崎　隆司[*3]
岡野　邦彦[*5]・笠井　雅夫[*4]・新谷　吉郎[*5]・畑山　明聖[*5]

（1987年6月8日受理）

主要物理設計の考え方を示す。それはプラズマ設計にとって重要な基盤であり，また炉設計概念にインパクトを与えるものである。設計思想を2つのグループ，物理設計ドライバーと物理設計条件に分けた。前者は設計者が自由に選択でき，設計者の考えに左右されるものであり，例えば自己点火，パルス長，運転シナリオなどである。後者は自然法則に従うものであり，閉込め，ベータ値限界，密度限界などがある。

那珂研究所：〒311-02 茨城県那珂郡那珂町大字向山801－1
＊1　外来研究員　㈱日立製作所
＊2　外来研究員　三菱電気㈱（現在 三菱電気）
＊3　㈱日立製作所
＊4　三菱原子力工業
＊5　㈱東芝

IV. Summary

The plasma design philosophies for the FY86 FER conceptual design are stated. They are classified into two groups, physics design drivers and physics design constraints, according to the feature whether or not a designer is free to choose his option. Twelve design drivers have been picked up and the choices for them are elucidated. Sixteen design constraints have also been evaluated and the guidelines for them are described.

Acknowledgements

The authers would like to express their appreciation to FER engineering design team members, especially Dr. H. Iida: a team leader, Dr. R. Saito: a group leader of a plant system group, Dr. T. Kobayashi : a leader of a reactor structure group, Dr. N. Miki: a group leader of a magnet group, and Dr. K. Nakashima: a group leader of a electrical group for their fruitful discussions.

The authors also would like to express their appreciation to Drs. S. Mori, K. Tomabechi, M. Yoshikawa, and S. Tamura for their continued support.

Contents

目　　次

I. Introduction

Japan Nuclear Fusion Council organized the Subcommittee on the Basic Issues of Fusion Development, August 1985. The Subcommittee studied basic principles for the nuclear fusion research and development programmes in Japan after the break-even plasma condition is achieved by JT-60. Based on the interim report worked out by the Subcommittee, it is considered appropriate to achieve self-ignition and long pulse burning and to conduct primary reactor engineering tests in the next step device, considering many aspects of nuclear fusion researches, such as the present status of nuclear fusion research and development, expectable results from large tokamaks including JT-60, pioneering characteristic as a research objective adequately compensating research investment for more than ten years after this, and problems that lie ahead awaiting solution before practicalization of nuclear fusion reactor.

Objectives of the next step device are, therefore, to accomplish missions stated below.

(1) As reactor core technologies mission, to achieve self-ignition including burn control and long pulse burning for a significant time span covering a current diffusion time.

(2) As reactor technologies mission, to develop and test tritium fuel cycle, superconducting coil, remote maintenance, and breeding test module blanket.

In addition to the above physics missions, i.e., achievement of a self-ignited plasma (physically equivalent to $Q \gtrsim 20$, Q: Fusion power multiplication factor) and stable control of plasma for a long time (more than current diffusion time of several hundred seconds), the following general guidelines for the design philosophy have been applied to the plasma design for FY86 FER.

(1) Considering the commencement of construction in near future (several years), adequately reliable data bases are chosen, although potential progress are also taken into consideration.

(2) Risks in achieving the missions stated above should be minimized as small as possible.

(3) Much attention should be paid on cost-effectiveness.

In this report, we describe the major physics design philosophies which are the essential bases for the plasma design and has also significant influences on a reactor design concept. Those design philosophies can be divided into two classes, design drivers (main physics features diving design concept) and physics design constraints. The design driver is a feature that a designer is free to choose. This choice may be guided by his opinion as to feasibility or drivability, but nevertheless he is free to make a choice. For example, to choose an ignited plasma is a design driver. On the other hand, the design constraint is a physical law and a designer is not free to choose whether or not to follow it. For the above example of ignition as a design driver, the enegy confinement scaling law is a design constraint.

In the next two chapters, we will describe the choices for the physics design drivers and the guidelines for the physics constraints selected for the FY86 FER plasma design, and discuss reasons why such selections are made.

The above classification into two groups, design drivers and design constraints, was discussed in the INTOR workshop for the critical analysis of existing INTOR-like devices like FER, NET, TIBER, and OTR. The contents described in this report is a part of our contributions to INTOR-related IAEA Specialists' meeting on Engineering Test Reactor national design concept, which was held March 23-27, 1987.

II. Physics Design Drivers

The physics design drivers, which may drive a design concept, are featured by the fact that a designer is free to choose his option, guided by his opinion. The following twelve physics design drivers items have been chosen for the FER plasma design.

DP 1 Fusion performance (Energy multiplication rate, Q)
DP 2 Burn pulse length
DP 3 Operation scenario
DP 4 Impurity and particle control method
DP 5 Plasma configuration
DP 6 Start-up assist
DP 7 Plasma heating methods
DP 8 Frequency of major disruptions
DP 9 Burn temperature control
DP10 Toroidal field ripple
DP11 Maximum impurity level
DP12 Fast α-particle confinement

In this chapter, we describe our choices for the above design drivers at first. In the remarks following each choice, many aspects accompanied with each choice are discussed.

DP 1 Fusion performance (Energy multiplication rate, Q)

[Choice for FER]

$Q \gtrsim (20\text{-}30)$

[Remarks]

The energy multiplication factor, Q is defined here as the ratio of nuclear fusion reaction output power to input power to reactor core plasma at the stage of burning.

Relations between physics issues on burning plasma and Q value necessary for them are shown in the following Table. It becomes clear that all physics issues on burning plasmas can be studied and will be clarified when Q value more than 20-30 is met.

Behaviours of α-particles may be investigated sufficiently using plasmas with Q of around unity. The studies of α-particle heating may need plasmas with Q more than five at least, because the α-particle heating could be studied under the condition that α-heating power is substantially governing in comparison with the external power, and Q=5 is the condition that α-heating power is equal to power added externally. The demonstration of burn temperature control will need plasmas with $Q \gtrsim 20$, where the α-heating power is completely leading.

Table Relations between physics research issues on burning plasma control and Q value

Item	Range of value	Research issues
Q value	$\gtrsim 1$	Behaviour of fast α-particle generated from nuclear fusion reaction
	$\gtrsim 5$	α-particle heating
	$\gtrsim 20$	Burning control

DP 2 Burn pulse length

[Choice for FER]

Around 800s

[Remarks]

Relations between burning time and research items on burning plasma control are shown in the following Table. The burning time of about 800s can cover all physics issues related to long pulse burning.

The α-heating physics could be studied with plasmas with burning time of a few second, because the slowing-down time of α-particles is less than a second. The demonstration of thermal instability control will need burning duration more than 10s, considering that the characteristic time of thermal instability is in a range of energy confinement time. To demonstrate capability of helium ash exhaust, it will take longer time, taking account of longer, though still unclear, particle confinement time and time necessary for helium to accumulate in plasmas and to approach a steady state. In addition, demonstration of reliable fueling may also be achieved in this time scale. The longest time scale is current diffusion time of several hundred seconds for INTOR-like plasmas.

Table Relations between physics research issues on burning plasma control and burning time

Item	Range of value	Research issues
Burning duration	$\gtrsim$ a few (sec)	α-particle heating
	$\gtrsim 10$	Thermal instability control
	$\gtrsim 100$	Helium ash exhaust and fueling
	~ 800	Current diffusion control

DP 4 Impurity and particle control method

[Choice for FER]

Poloidal divertor with single null.

[Remarks]

Two options, divertor and pumped limiter, are realistic candidates for impurity and particle control for the next step device. The present data bases and numerical studies for them clearly show superiority of a poloidal divertor to limiter option, in achieving low temperature and high density plasma, which may be the sole solution at present to avoid the high erosion of the target plate in long burning. The poloidal divertor option is also consistent with an assumption that favourable confinement like the so-called H-mode will be achieved in FER plasmas.

There is some possibilities to use a limiter option, e.g., at a plasma initiation stage and a plasma current startup stage. The operation scenario at those stages has not been fixed yet, because there are still large uncertainties in possibility to operate high-recycling and low-temperature divertor operation at the current rampup stage due to requirements of rather low-density operation. Further studies and experiments are needed

There is still some room for selecting single-null or double-null configuration. The selection may have little impacts upon performance of impurity and particle control, and it needs more overall judgement on design concept. It will be remarked in plasma configuration.

DP 3 Operation scenario

[Choice for FER]

Scenario is a pulse operation using a hybrid of inductive and non-inductive current drive. Plasma current is sustained inductively at a stage of burning, and plasma current is ramped up mainly by a non-inductive current drive method.

[Remarks]

A variety of operation modes have been compared from conventional fully-inductive pulse operation to non-inductive steady state operation. Those comparative studies include the followings;

(1) effects of the OH flux swing range upon facility size,

(2) data bases at present on non-inductive current drive and their expansion that can be expected in the near future,

(3) steady state operation of tokamak types by highly efficient non-inductive current drive.

From those studies, the followings have been confirmed;

(1) it is not the best way to rely fully on the inductive method even at the stage after JT-60, since steady state operation and compact facility will be extremely important.

(2) higher efficiency and profile controlability can be expected if research and development on non-inductive method be made sufficiently.

Based on those points, it has been decided that operation mode should be pulse operation with burning time for about 800s. A non-inductive method and an inductive method should be mainly employed for current rampup and for current sustaining, respectively. In addition, at the time when function of non-inductive method proved higher than presently assumed, the facility may be built more compactly. It is also required that experiments to achieve steady state operation should be undertaken at the phase of facility operation as one of the important tasks.

DP 5 Plasma configuration

[Choice for FER]

Plasma shape is defined by a magnetic surface having a 95% flux. Its elongation and triangularity are κ =1.7 and δ =0.2, respectively. The outermost surface dividing a main plasma from scrape-off plasma has a single magnetic-null point.

[Remarks]

Plasma configuration correlates with a lot of critical issues, e.g., vertical positional stability of plasmas, critical beta value, probably energy confinement time for physics, and access philosophy for maintenance and power supply for poloidal coils for engineering. The higher elongation may be favourable for high performances of critical beta and energy confinement. The highly elongated plasma, however, becomes very unstable vertically and is not easily stabilized for INTOR-like reactor structures, which will limit the elongation. Studies on plasma positional stabilization have shown that the elongation of around 1.7 will be marginal by using reasonable passive shell structure and reasonable capacity of power supply and location for control coils.

The selection of single- or double-null configuration is also related to poloidal coil system and maintenance philosophy. For dee-shaped plasmas, highly elongated plasmas with double-null configuration are favourable in reducing the power supply of poloidal coils, which are arranged to vertical access for maintenance. On the other hands, mildly elongated plasmas of about 1.7 elongation with single-null configuration minimize the power supply of poloidal coils, which are arranged to horizontal access. Furthermore, the horizontal access seems remarkably superior to vertical access for maintainability.

Based on those studies, the mildly elongated single-null configuration has been selected, with the horizontal access.

In our plasma equilibrium studies, we use three types of noncircularity (elongation and triangularity). The first one (κ, δ) is defined on the magnetic surface with 95% flux, and is used in other areas, such as plasma specification and system code

studies. The second (κ_N, δ_N) is defined at magnetic null points. The third one (κ_S, δ_S) is defined on the separatrix surface.

From experiences on plasma equilibrium studies, the following relations are derived between (κ, δ) and (κ_N, δ_N).

For double-null configuration,

$$\kappa_N = 1.24\kappa - 0.13,$$
$$\delta_N = 1.52\delta - 0.085.$$

For single-null configuration,

$$\kappa_N = 1.24\kappa_1 - 0.13,$$
$$\delta_N = 1.52\delta_1 - 0.085.$$

where,

$\kappa_1 = 1.2\kappa$, $\delta_1 = 1.4\delta$ on the side with null,

$\kappa_2 = 0.8\kappa$, $\delta_2 = 0.6\delta$ on the side without null.

The noncircularity (κ_S, δ_S), defined on the separatrix, therefore, is as follows.

For the double-null case,

$$\kappa_S = \kappa_N, \quad \delta_S = \delta_N.$$

For the single-null,

$$\kappa_S = (\kappa_N + \kappa_2)/2, \quad \delta_S = (\delta_N + \delta_2)/2.$$

DP 6 Start-up assist

[Choice for FER]

Electron cyclotron wave of its power 3MW is used at the initiation stage of operation for pre-ionization and pre-heating of plasmas. The ordinary mode with the frequency of fundamental harmonic will be launched from a low toroidal field side.

[Remarks]

In the FER operation scenario, plasma current will be ramped up mainly non-inductively. Details of startup scenario are still open, because it depends on non-inductive current drive methods and it has still uncertainties. One reliable scenario is to use conventional inductive method at a just initial stage, i.e., plasma current is ramped up inductively to about 0.5MA with an aid of EC wave. The use of EC wave with a reasonable power 3MW is adequate to reduce initial loop voltage and to save OH flux.

Constraints from reactor structure cause a launcher system from a low field side and ordinary mode with the frequency of fundamental harmonic.

DP 7 Plasma heating methods

[Choice for FER]

Many options are now being deliberated and a final selection seems too early. Typical options are as follows;

(1) Ion cyclotron wave, especially 2nd harmonic for deuterium, in addition to lower hybrid wave for current drive,

(2) Neutral beam with its energy range 250-500keV, which is used for heating and current drive.

[Remarks]

Heating components seem to be loosely coupled with reactor structure, even in a tangential NB heating case, unless a reactor size becomes too compact. Therefore, the postponement of selection of heating options has small impacts on reactor design concept, and the final selection is too premature because of uncertainties in heating and related physics.

The more crucial point to be studied for FER, which uses non-inductive current drive, is the common use of systems for heating and current drive to reduce power supply requirements and to simplify both systems. From those viewpoints, the above two typical options have been chosen as a tentative reference method, considering present data bases.

The tangentially injected NB with its energy range 250-500keV is a promising and realistic option, although some problems resulted from beam pressure during current drive have to be resolved. The IC wave is the leading heating option among RF heating options, and LH wave, which is also the realistic option for current drive, is used for heating approach in combination with the IC wave, while the LH wave has some uncertainties in heating performance.

The most realistic heating scenario for FER may be a combination of NB and LH, although it will make systems somewhat complicated.

DP 8 Frequency of major disruptions

[Choice for FER]

5% for 1st and 2nd operation phase and 1% for 3rd operation phase.

[Remarks]

In order to minimize development costs and technical risks, the phased operation concept will be adopted for FER and the machine will raise its performance step-by-step conducting careful check and review. The whole operation period is divided into the following three phases;

(1) Facility function confirmation phase (1～2 years, about 5000 shots), where facility functions are confirmed whether it works sufficiently as expected by using hydrogen and deuterium plasma.

(2) Burning experiment phase (1～2 years, about 1000 shots), where self-ignition is achieved by deuterium and tritium plasma and physics of burning plasma is also expected to be clarified.

(3) Full-rating operation phase (5～6 years, about 12000 shots), where long pulse burning for about 800s is achieved in this phase and thereby high availability operation is intended.

The first two phases differ substantially from the last one, in terms of disruption frequency. In the first two phases, plasma performance is increased step by step with developing new operation regions, while they are within expected performance. On the other hand, in the last phase, the full-rating operation, which is confirmed at the end of the second phase, will be repeated. The frequency of major disruptions for the first two phases is surely expected higher than that of the last phase, although their quantification is very difficult. The above choice for the frequency of major disruptions is not completely based on data base, however, it is considerably severe compared with the INTOR specification.

DP 9 Burn temperature control

[Choice for FER]

Not specified.

[Remarks]

Thermal equilibrium of D-T burning plasmas depends upon power balance between α-particle heating and whole power losses from plasmas. In the next step device, its operating average temperature is usually set to around 10keV, from the viewpoint that plasma performance, represented by energy multiplication factor Q, is maximized within the allowable beta limit. Such a temperature region is thought unstable thermally, although confinement degradation near the beta limit, if it is not disruptive, may be helpful to stabilize the thermal runaway.

Various methods for controlling the thermal instability have been proposed so far. Typical candidates are (a) compression/decompression, (b) variable toroidal field ripple, (c) fuelling/exhausting, (d) beta value limit, (e) sub-ignition operation. For each method, a lot of studies have been made up to now.

Those candidates have also been evaluated and compared among them from various viewpoints, such as physics mechnisms to be clarified, control technologies and their applicabilities, requirements to diagnostics, and impacts on reactor design. Most of the candidates and their combination seem to have potential in application to the next step device, while, it is too premature to select the reference option at present, because of large uncertainties. Further developments are necessary. First of all, the energy confinement scaling must be confirmed for plasmas in large tokamaks like JT-60. Experiments simulating the thermal instability control in JT-60 are also important. Experimental data bases on α-particle behaviour from JET and TFTR are quite crucial for the final decision.

DP10 Toroidal field ripple

[Choice for FER]

0.75% at plasma edge.

[Remarks]

The ripple value of toroidal field is dependent upon toroidal coil size and number, which is also correlated to maintenance philosophy and poloidal coil system including power supply, although the ripple value can be reduced by means of feromagnetic materials inserted in toroidal coil bore. Problems related to the toroidal ripple are α-particle loss and heat load on first wall. Those problems have been evaluated numerically using Monte-Carlo method so far, i.e. by K. Tani and L.M. Hively. There are however some discrepancy in both results, that is, Tani's results are around three times larger than Hively's. Efforts to clarify the reason of the discrepancy are continued, and clear results have not been obtained yet.

Our selection for the toroildal ripple is based on the Tani's results. The ripple of toroidal field, δ is defined as

$$\delta = \frac{B_{max} - B_{min}}{B_{max} + B_{min}}.$$

δ =0.75% has been selected for FER. Even for such relatively small ripple, compared with the INTOR specification, the α-particle loss power amounts to about 10% of the α-heating power. Futhermore, Tani's calculations show that the heat load on the first wall is significantly localized under each toroidal coil near the midplane, which reflects the fact that the ripple enhanced banana drift loss is the dominant loss mechanism, and show that the peak heat load reaches 0.8-0.4MW/m^2. When the peak heat load is too high, the ripple insert mentioned above should be used to reduce the peak heat load below the allowable level.

DP11 Maximum impurity level

[Choice for FER]

Effective ionic charge, Z_{eff}=1.5, at burning stage. At a startup stage impurity level will be increased and Z_{eff} depends on operation scenario and current drive options.

[Remarks]

Plasma purity should be kept during burning. Generally speaking, the allowable impurity level is 1% for light impurities, 0.1% for medium metal impurities, 0.01% for heavy metal impurities. For burning plasmas, high-recycling and low-temperature divertor plasmas may be expected in the light of present data bases. The burning plasmas are therefore assumed to be contaminated only with light impurities and the maximum impurity level is assumed that the effective ionic charge is Z_{eff}=1.5. The typical concentration for ions is assumed to consist of 46.5% for deuterium and for tritium, 5% for helium, 1% for hydrogen, 0.5% for carbon and for oxygen.

On the contrary, during the startup stage, impurities can be introduced, intentionally in some cases, to optimize a startup scenario and consequently the impurity level depends upon the scenario. The impurity level of the startup stage may therefore differs in different current drive methods. For the startup scenario using mainly NB, plasmas of rather high density with Z_{eff}=10 will be utilized to shorten rampup time by adding inert gases like Ar or Xe. For a LH startup case, an appropriate impurity level should be determined to optimize the rampup scenario with taking account of the impurity production and shortening the rampup time.

DP12 Fast α-particle confinement

[Choice for FER]

Power loss due to direct fast α-particle loss should be limited less than 10% of α-heating power.

[Remarks]

The fast α-particle loss has significant impacts on plasma power balance. The anormalous radial diffusion of fusion α-particles, which have been studied quantitatively, may be limited to the α-particle loss due to the toroidal field ripple. According to the numerical calculations by K. Tani, the field ripple 0.75% causes power loss corresponding to around 10% of α-particle heating power, which may have a large influence on plasma power balance. Additional power loss due to other unspecified mechanisms should therefore be as small as possible. The power loss related to the field ripple can be reduced by reduction of field ripple with the aid of ripple inserts with keeping toroidal coil size, when the whole power loss related to fast α-particle confinement becomes too large.

III. Physics Design Constraints

Physics design constraints are featured by the law of nature and a designer is not free to choose whether or not to follow it. We have picked up the following sixteen physics design constraints for ths FER plasma design.

CP 1 Plasma confinement
CP 2 β-limit
CP 3 β_{total}/β_{DT}
CP 4 q-limit
CP 5 n-limit
CP 6 Fusion power density
CP 7 Plasma temperature
CP 8 Inductive loop voltage
CP 9 Plasma edge and scrape-off conditions
CP10 Impurity release and erosion rate
CP11 Disruption scenario
CP12 Particle exhaust and fuelling requirements
CP13 Power deposition efficiency and profile
CP14 Current drive efficiency and profiles
CP15 Parameter ranges for heating and current drive
CP16 Plasma heating power flow

In this chapter, the guidelines, which should be followed by a plasma designer, are stated at first for each design constraint for the FER plasma design. In the remarks following each guideline, some considerations and discussions are presented for better understanding the guidelines for the design constraints.

CP 1 Plasma confinement

[Guideline for FER]

Mirnov-type scaling law for global energy confinement time, $\tau_E^{Global}[s] = 0.155a[m]I_p[MA]\sqrt{\kappa}$, is applied to zero-dimensional power balance anlyses with an ignition margin of unity, where κ is plasma elongation.

[Remarks]

The Mirnov-type scaling for global energy confinement time has been derived from experimental data of devices operated with divertor configurations, such as JFT-2M, ASDEX, PDX, and Doublet III. Some details are described in Appendix.

Uncertainties in extrapolating the energy confinement scaling to the INTOR-like devices however seem still quite large. For instance, the latest experimental data from JFT-2M show weak dependence of plasma current at high current region, and an another scaling, $\tau_E^{Global}[s] = 0.046a[m]R[m]B_T[T]\sqrt{A}$, seems more appropriate for fitting experiments. The application of such a scaling to the FER design, instead of the Mirnov-type one, yields the almost same results, although the new scaling is slightly unfavourable for plasmas with a smaller major radius, because of its R-dependence. Further intensive studies for deeply understanding energy confinement performance are therefore urgently requested, especially parametric studies in a wide range for high-temperature plasmas with good confinement in large tokamaks.

[Appendix] "Energy confinement time scaling law for FER"

Experiments in medium-size tokamaks with divertor configurations show that energy confinement time during additional heating almost keeps the value for Ohmic heating, or the degree of degradation in confinement is not severe, under some limited condition (the so-called H-mode operation), and fortunately, large tokamaks, JET and TFTR, have lately been succeeded in reproducing H-mode plasmas and good confinement plasmas called supershot, respectively. The experimental data, which have been obtained parametrically in the medium-size tokamaks for a couple of years, disclose that the global energy confinement time is strongly dependent

upon plasma current, non-circularity (elongation), and input power, while it is almost independent of density and magnetic field. Those experimental observations, obtained from ASDEX[1], PDX[2], DIII[3,4], and JFT-2M[5], are summarized in Figure as a relation between the global energy confinement time normalized by the product of plasma current and square root of plasma elongation ($\tau_E/I_p\sqrt{\kappa}$) and the total input power. The confinement time classified into the H-mode scatters in a relatively wide range, and seems to be continuously connected to the so-called L-mode with degradated confinement time. Especially, in PDX τ_E is strongly deteriorated in a range of a large input power. The speculated reasons are; (1) the level of edge relaxation phenomena might increase, (2) excess gas fuelling for avoiding disruptions could interrupt entering the H-mode region.

In DIII experiments, the normalized confinement time $\tau_E/I_p\sqrt{\kappa}$ has tendency that divertor discharges have superior confinement time to limiter discharges, although the former data overlap the latter ones, and they are shown by open circles. The normalized confinement time decreases gradually with the power and seems to have the tendency to be saturated. Those data have been fitted with two ways, $(a + b/P_T)$ and cP_T^{-d}, with a=0.044, b=0.059, c=0.097, and d=0.35. Both fittings can reproduce experimental data within the same accuracy, and there is nothing to choose between two in a range of the available experimental data. Assuming the former way of fitting and the input power is quite large in a next step device, the Mirnov-type scaling law can be derived,

$$\tau_E[s] = 0.155a[m]I_p[MA]\sqrt{\kappa} .$$

Here, the confinement time is normalized by the minor radius of DIII plasmas to get a Mirnov-type scaling law. Furthermore, the confinement time is enhanced by $\sqrt{2}$, taking into consideration that in most devices the confinement time is improved by a factor of 1.5～2.0 with deuterium plasmas, compared with hydrogen ones.

On the other hand, ASDEX reveals that the confinement is independent of the input power, after a clear transition from L-mode to H-mode, and the same results are also obtained in JFT-2M. Those results disclose that the confinement time can be recovered to a level of Ohmically heated one, when the H-mode transition occurs. Both experiments, however, cover only a small range of the power, and further studies with enhanced heating

power are urgently requested. The closed divertor configuration in ASDEX may be favourable in realizing the clear transition to the H-mode, however it is not a absolute necessary condition, considering that JFT-2M observes the H-mode with open-type divertor, as well as DIII, and lately Big DIII and JET.

Most of those H-mode plasmas are observed in discharges with NB heating. IC heated plasmas are somewhat difficult to transit into the H-mode, because the formation of a temperature pedestal, observed in most transitions to the H-mode, may be interrupted by introduction of impurities from RF launchers or first wall. Lately, however, ASDEX and JFT-2M have been succeeded in obseving the H-mode in IC heated discharges, although heating power for transition is higher than that for NB discharges. No essential difference seems to exist among various heating methods, although the H-mode transition in LH heated plasmas has not been observed yet.

One necessary condition for H-mode transition is the formation of edge pedestal in temperature, as mentioned above. It generally requires the suppression of excess recycling of neutral particles near the edge, which could be easily realized in divertor configurations. Moreover, H-mode plasmas might be accompanied inherently with reduced transport near the edge, while the essential trigger of the H-mode has not been identified yet.

The interesting evidence from JFT-2M is the observation of H-mode plasmas in limiter discharges, which needs a special recipe for the H-mode transition. The H-mode with limiter discharges is not robust and is easily interupted during a pulse. It is therefore too premature to apply the H-mode concept with limiters to the next step device design.

References

[1] A. Staber et.al., Proceedings of the 4th International Symposium on Heating in Toroidal Plasmas, Rome, 1984 (ENEA, Frascati, 1984), Vol.1.

[2] R.J. Fonck, et al., ibid., Vol.1, p.37.

[3] J.C. Deboo, et al., Nuclear Fusion 26 (1986) 211.

[4] A. Kitsunezaki, et. al., in Plasma Physics and Controlled Nuclear Fusion Research, Proceedings of the 10th International Conference, London, 1984 (IAEA, Vienna, 1985), Vol.1, p.57.

[5] N. Suzuki, private communications.

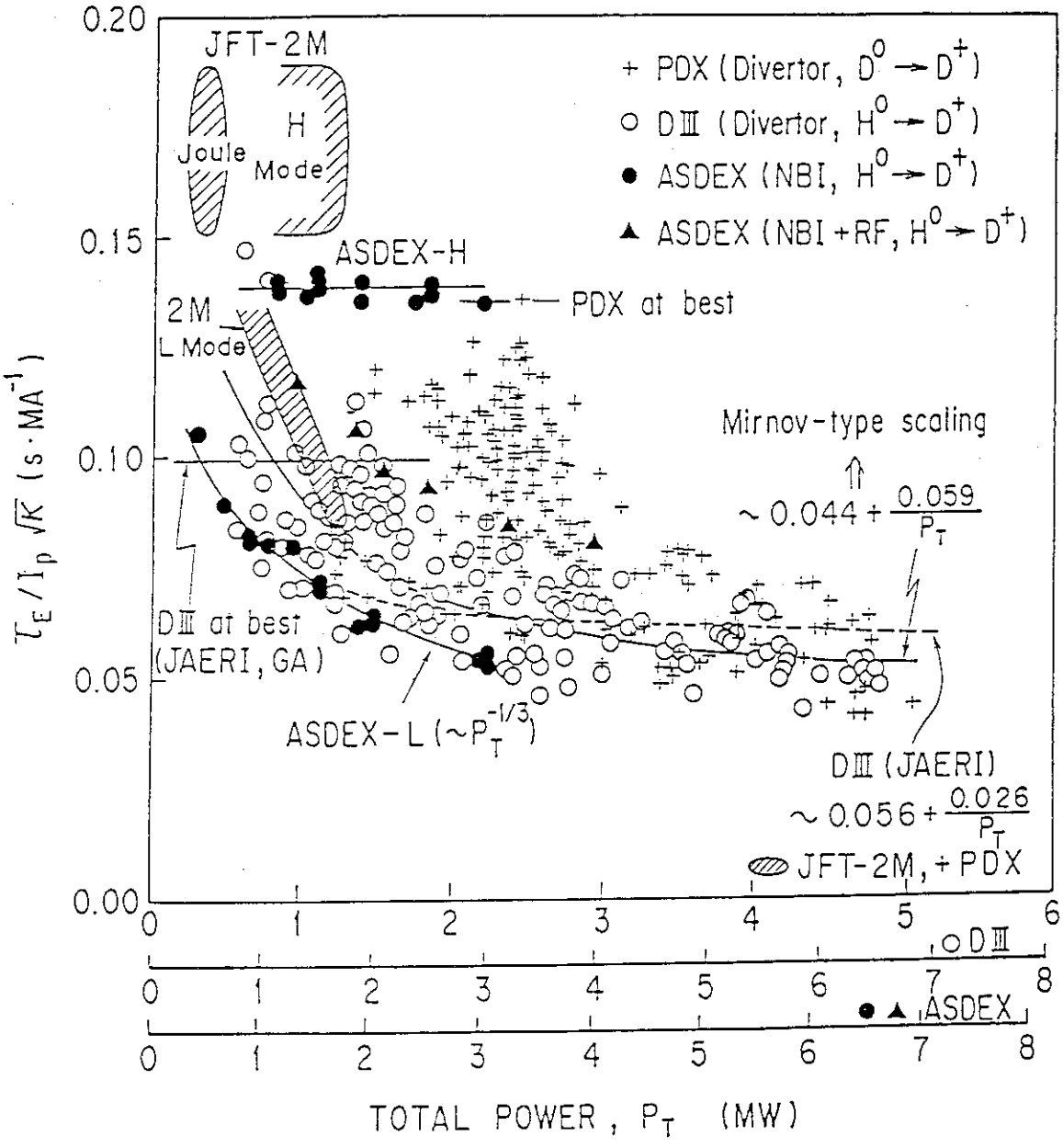
JFT-2M
Joule
H Mode
+ PDX (Divertor, $D^0 \rightarrow D^+$)
○ DⅢ (Divertor, $H^0 \rightarrow D^+$)
● ASDEX (NBI, $H^0 \rightarrow D^+$)
▲ ASDEX (NBI+RF, $H^0 \rightarrow D^+$)
ASDEX-H
PDX at best
2M L Mode
Mirnov-type scaling
$\sim 0.044 + \frac{0.059}{P_T}$
DⅢ at best (JAERI, GA)
ASDEX-L ($\sim P_T^{-1/3}$)
DⅢ (JAERI)
$\sim 0.056 + \frac{0.026}{P_T}$
JFT-2M, + PDX
$\tau_E / I_p \sqrt{K}$ (s·MA^{-1})
0.20
0.15
0.10
0.05
0.00
0 1 2 3 4 5 6
○ DⅢ
0 1 2 3 4 5 6 7 8
● ▲ ASDEX
0 1 2 3 4 5 6 7 8
TOTAL POWER, P_T (MW)

CP 2 β-limit

[Guideline for FER]

Troyon-type scaling, $\beta[\%] = 3.5 I_p[MA]/a[m]B_T[T]$, is used for the limit of averaged toroidal beta value.

[Remarks]

The Troyon-type scaling can well follow experimental and numerical results, belonging to 1st stability region. Access to the 2nd stability region, which is successfully demonstrated in theoretical and numerical studies, has not been observed in experiments. It is therefore too risky to apply 2nd stability concept to plasma design of the next step device at present, although the improvement in the allowable beta seems to have great potential, when a plasma current density profile could be tailored, e.g. by non-inductive current drive method. The numerical factor, 3.5, also seems to be correlated to a safety factor, which is discussed in Appendix.

[Appendix] "Parameter space for β-limit and safety factor"

As far as the β-limit is concerned, the Troyon-type scaling

$$\beta[\%] = G\frac{I[MA]}{a[m]B[T]}$$

has been widely confirmed to approximately explain both of experimental data and numerical results with $G=3\sim4$. The range of the numerical factor, G is dependent upon experimental conditions and especially it receives tight constraint by plasma disruptions. Experimental evidences from ASDEX, DIII, and JFT-2M are summarized on a G-q_* plane in Figure, in which a region for disruptions is also indicated, where q_* is the safety factor approximated by a ellipsoidal cylinder. The figure clearly shows that plasma disruptions limit the operation region of the allowable beta and the safety factor, and that the low-q_*, high-beta operation is quite difficult due to plasma disruptions. E.g., in ASDEX, G=4 is observed with $q_* \gtrsim 3$. The DIII results also show that such a tendency is more evident in a divertor operation than in a limiter operation. Based on such experimental observations, the following two directions are available for possible selection for a combination of G and q_*, (1) relatively high q_*

and large G, (2) low q_* and small G. The latter choice may be preferable for the next step device, because plasma performance is propotional to the product of τ_E and β, which is resultantly propotional to GI_p^2 or Gq_*^{-2}. Based on those considerations,

$$G = 3.5, \quad \text{and} \quad q_\psi = 2.6 \ (q_* \simeq 2)$$

is selected for FER plasma design.

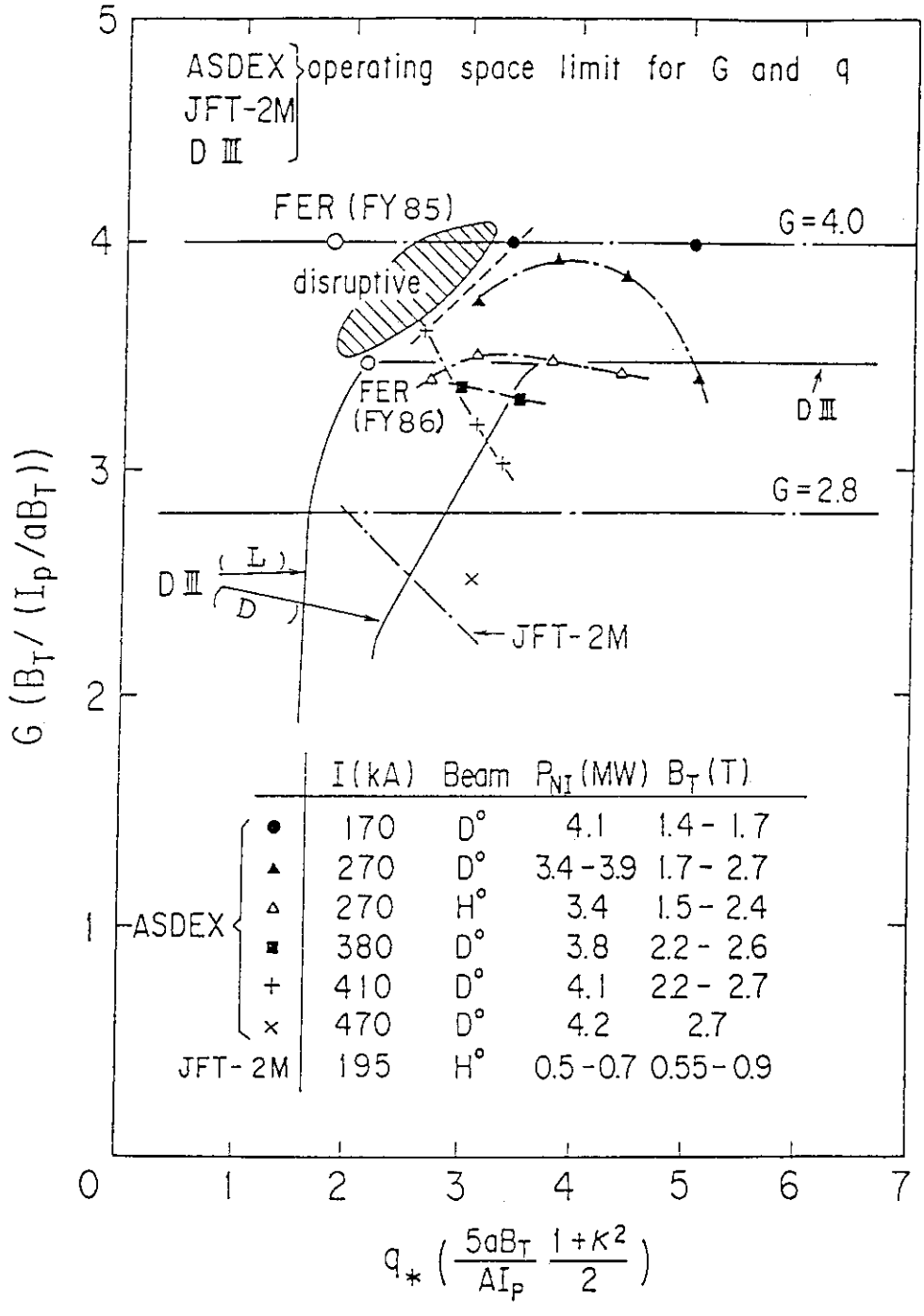

CP 3 β_{total}/β_{DT}

[Guideline for FER]

Total beta value consists of contributions from electrons, fuel D/T ions, impurity ions, thermal helium ions, fast α-particles, and fast neutral beam particles. The typical concentration for ions is assumed as follows: 46.5% for deuterium and for tritium, 5% for thermal helium, 1% for hydrogen, 0.5% for carbon and for oxygen. Those percentages result in Z_{eff}=1.5. The fast α-particle contribution is estimated by an enhancement factor, (1.0 + (0.015T[keV] - 0.1)) in a temperature range, 7keV$\lesssim$T$\lesssim$30keV. The fast neutral beam contribution can be calculated from an orbit following Monte-Carlo code or an analytical solution of Fokker-Planck equation.

[Remarks]

The total beta value, β_{total} can be expressed as,

$$\beta_{total} = \beta_{DT} + \beta_{He} + \beta_{Imp} + \beta_{\alpha} + \beta_{NB}.$$

The enhancement factor of the fast α-particle contribution, which is the approximation of the Jassby's analysis, is defined as the ratio of the α-contribution to the whole beta value of thermalized particles, i.e.,

$$\beta_{\alpha} = \beta_{bulk}(0.015T[keV] - 0.1),$$

$$\beta_{bulk} = \beta_{DT} + \beta_{He} + \beta_{Imp}.$$

Considering the Jassby's result, which does not include the effect of impurities, it seems more reasonable that the enhancement factor is defined as the ratio of β_{α} to the sum of $\beta_{DT} + \beta_{He} + \beta_{Imp}$. For the above impurity condition, however, the difference is quite small.

The burning plasma consisting of the above ingredients has the following characteristics;

the ratio of electron to ion densities:	1.11
the ratio of electron to DT ion density:	1.19
the effective ionic charge:	1.48

For a typical condition of burning plasmas with T_e=T_i=12keV, the ratio of β_{total} to β_{DT} is 1.23.

The β_{NB} contribution is of significance. E.g., when the NB

current drive option is applied to the startup stage, the β_{NB} is the main contributor and may play a crucial role in optimization of the startup scenario. For a steady state reactor sustained by NB current drive, which is not the FER reference option, the β_{NB} contribution will also occupy a significant part of the total beta, and it will reduce the power multiplication factor, although such a problem will be eased by improvement in the critical beta value.

CP 4 q-limit

[Guideline for FER]

q_ψ =2.6-2.8 is selected for MHD safety factor.

[Remarks]

The safety factor correlates with the allowable beta value, energy confinement time, power supply for poloidal coil system, α-particle confinement, and plasma disruptions.

The allowable beta value, which has been postulated to follow the Troyon-type scaling as mentioned in the β-limit constraint, is improved with the lower safety factor, because β-limit scales in proportion to I_p. The energy confinement time is also enhanced due to the linear dependence upon I_p of the Mirnov-type scaling, selected for FER plasma design. Those favourable dependences on I_p ensure the plasma size reduction with the lower safety factor selection.

As far as the α-particle absolute confinement is concerned, several MA current is enough to confine high energy α-particles, and such a condition is almost always satisfied with all INTOR-like designs. On the other hand, the currents through poloidal coils approximately propotional to plasma current, and the lower safety factor will lead to the increase of the power supply of the poloidal coil system. The lower safety factor therefore is not sure to bring the overall cost effectiveness, and carefull analyses may be needed.

The operation region of lower safety factor is also severely limited by plasma disruptions, as mentioned in the remarks of the β-limit. The operation with MHD $q_\psi \simeq 2.0$ seems extremely difficult for INTOR-like machine, although stable discharges with $q_\psi < 2.0$ have been successfully observed in some rather small-size machines. Especially, the low-q_ψ operation with high β state with divertor configirations has never been observed in any tokamaks, as mentioned in the remarks of the β-limit.

Considering those situations, the following selection is made for FER plasma design,

q_ψ = 2.6-2.8.

CP 5 n-limit

[Guideline for FER]

The n-limit is not thought to be a strong constraint in FER plasma design. Namely, plasma is designed without the density constraint, and the resultant density is checked by the present database, e.g., $\bar{n}_{e,max}[10^{20}m^{-3}]=1.5B_T[T]/R[m]$ during a burning stage.

[Remarks]

In general, most of experimental results follow the so-called Murakami-scaling, $\bar{n}_e = C_n B_T/R$, which was proposed empirically almost ten years ago. Since then, the numerical factor C_n has been improved remarkably by means of improving the level of plasma purity and increasing heating power. The evolution of improvement of the density limit still continues. In the burning stage of FER plasmas, the conditions for the density limit may not be severe, because burning plasmas are postulated to be rather clean and the α-heating power is quite large.

The impurity level is assumed $Z_{eff}=1.5$, contaminated with 5% for helium, 0.5% for carbon and for oxygen, with expecting an excellent divertor function with high-recycling and low-temperature characteristics. Reflecting those choices, the density limit during the burning stage is not taken seriously as a limiting factor in the plasma design, and the resultant density is just checked in the light of the present data bases. Even if the resultant density would be beyond the present data, the excessed density, if it is not too large, will be accepted for FER design, because the improvement in the density limit is anticipated convincingly.

During the startup stage, some attentions should be paied on the density limit. The non-inuctive current drive option has been applied to the FER design concept. The operation density will be rather low, around $1.0\times10^{19}m^{-3}$, but the impurity level will be raised to optimize the startup scenario, e.g., a startup with NB current drive might need $Z_{eff}=10$ with Xe impurities. The data base for the density limit in such dirty plasmas is scarce, and careful attentions should be paid to it.

CP 6 Fusion power density

[Guideline for FER]

Fusion power is calculated from a formula, $1.5\bar{n}_D\bar{n}_T \langle \sigma v \rangle E_f$, where a numerical factor 1.5 reflects the effect of profiles of density and temperature, which are expected to be rather flat and rather round like parabolic, respectively.

[Remarks]

Fusion power is significantly dependent upon profiles of plasma density and temperature, and it gives large impact on plasma power balance and resultantly plasma size. Different profiles of density and temperature give different curves for ignition, as shown in Figure and Ref.[1]. The total fusion power increases by a factor of $1.5 \sim 2.5$ in a temperature range of 1-100keV, compared with uniform density and temperature profiles. The more peaked profiles are favourable for getting the large total power. It is not easy to predict the plausible potential profiles in the next step device, because of large uncertainties in thermal and particle transport characteristics. The most probable profiles, which may be reasonable guess from the present data bases, are a rather flat profile for densities, and a rather round profile for temperatures. Based on such an assumption, the fusion power is enhanced by a factor of 1.5 from the uniform profile case.

Referece

[1] M. Sugihara, et.al., JAERI-M 8621 (1980).

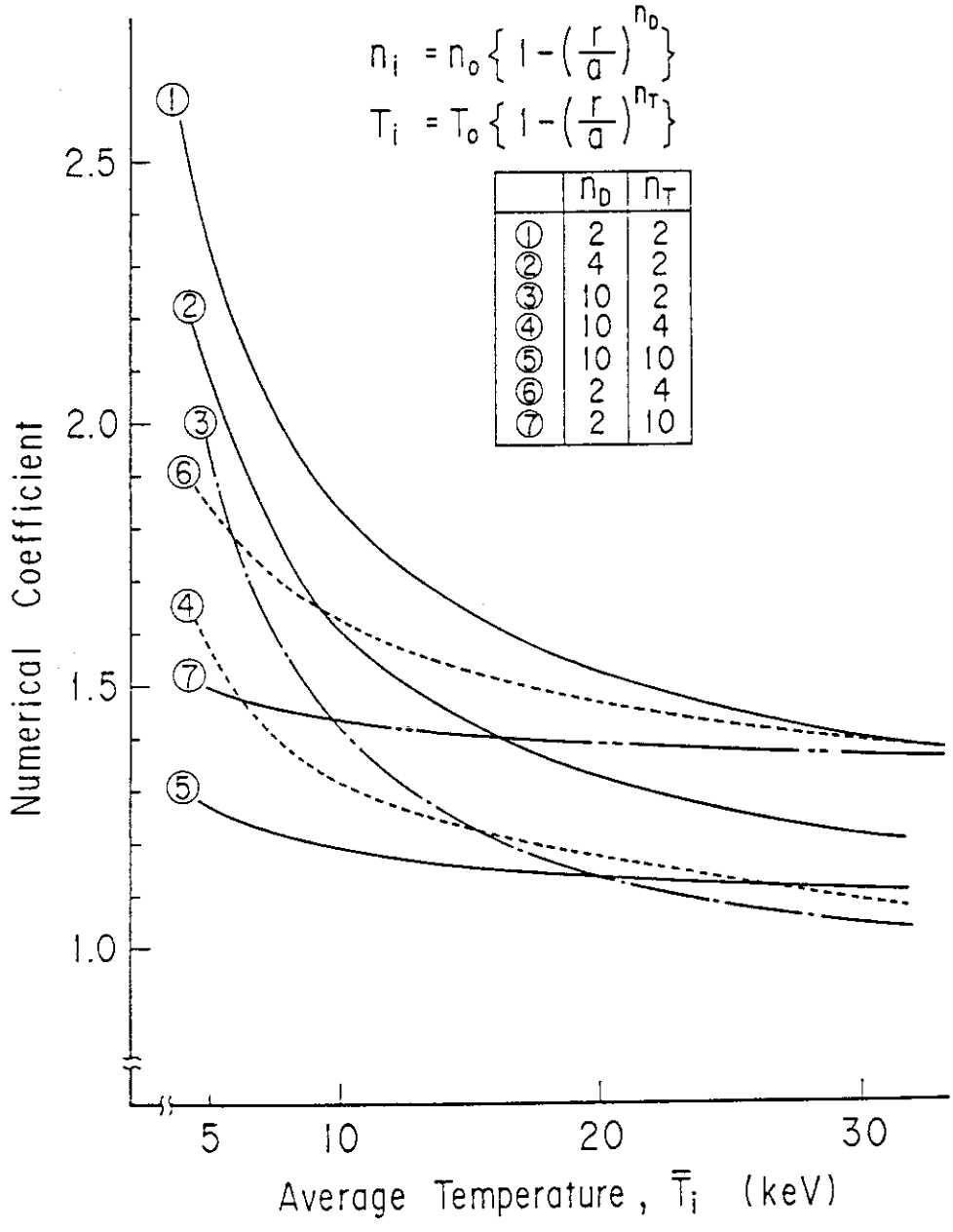

Fig. Dependence of required $\bar{n}\tau_E$ value for self-ignition on the distributions of density and temperature.

CP 7 Plasma temperature

[Guideline for FER]

$\bar{T}$[keV]/a[m] could be limited to less than 20.

[Remarks]

Plasma temperature profile will be produced as the results of power balance between α-heating power density and loss profiles mainly due to thermal transport, and therefore temperature profile will not be able to be freely selected.

Thermal transport physics are still very controversial and has large uncertainties, especially in an electron transport area. One interesting interpretation for present data bases is the so-called profile consistency, i.e. an electron temperature profile for a main confinement region hardly change in spite of a variety of heating profiles and methods. If it were a fact, the temperature profile could be severely limited in a reactor-grade tokamak.

The burning plasma will be operated near the β-limit, which is also a significantly severe constraint at present, and pressure profiles near the β-limit have a small room for changing themselves. This fact then imposes a strict constraint on temperature profiles.

Considering those situations, the temperature profile of burning plasmas may be allowed to take a quite limited one and almost uniquely determined. A most probable prediction of profiles from the present data bases might be a rather flat one for densities and a round profile like parabolic for temperatures, as mentioned in the remarks of fusion power density. The above limit is a crude value, derived from a lot of numerical studies on the β-limit.

CP 8 Inductive loop voltage

[Giudeline for FER]

Spitzer's formula is used for plasma resistivity.

[Remarks]

Inductive loop voltage is directly coupled with a part of transformer flux to be prepared for a burning period. Especially, for a design with a hybrid use of non-inductive current drive during a startup stage and inductive drive mainly during a burning stage, the evaluation of inductive loop voltage has substantial impact on the amount of the transformer flux, which resultantly influences reactor size and overall cost.

Two typical kinds of resistivity are proposed theoretically, i.e., a classical resistivity (Spitzer's one) and a neoclassical resistivity. For INTOR-like plasmas, the neo-classical resistivity is almost twice the classical one. The fact then yields big difference in the evaluation of the required flux for the transformer in the FER design.

The present data bases have still uncertainties, and it has not yet been able to take the reasonable one. JT-60 has observed that its plasma resistivities have no discrepancy with the Spitzer's one [1], although plasmas are still in the L-mode regeme and not in high-β region. Lately JET insists that plasmas have the neo-classical resistivity, while JET proposed the classical one before. TFTR has recently succeeded in reaching a high-β region, where it has observed a neo-classical effect, i.e. bootstrap current, although the observation is still quite preliminary because of limited measurements. Naturally, the plasma resistivity of TFTR should be neo-classical.

The Spitzer's resistivity has been selected for FER plasma design. Careful check and review for plasma resistivities should be continued further.

References

[1] T. Hirayama, et al., JAERI-M 87-029(1987).

CP10 Impurity release and erosion rate

[Guideline for FER]

The following conditions are considered as main constraints.

(1) A main part of charged particles flowing out from a main plasma is expected to go to divertor targets. The first wall, which is adequately apart from the separatrix, e.g., the separatrix-to-wall distance of a few times of density decay length, will receive a very small part of ions.

(2) Operation of a poloidal divertor in the localized recycling regime will cool the local plasma and reduce the energy of the incident ions. The temperature in the vicinity of the divertor plate will be decreased to less than 20eV.

(3) The main location of impurity release and of erosion by ions and charge exchange neutrals will be limited to the divertor targets and the first wall near the divertor targets.

(4) The maximum flux of charge exchange neutrals is $1.0\times10^{22}m^{-2}s^{-1}$ on the first wall near the divertor plate, and their incident energy is 60eV.

(5) The ingredients of incident ions to the divertor target consist of ions with the same concentration as the main plasma and sputtered impurities, the charge of which is assumed around 4.

(6) Dominant release of impurities appears due to physical sputtering.

(7) A large part of sputtered impurities are assumed to be confined within the divertor region and to be redeposited upon the divertor target.

(8) Impurity release and erosion during startup may differ significantly from the above, because of probable changes in scrape-off plasmas. Details have not been specified yet.

[Remarks]

Most of constraints related to impurity release and erosion rate are directly dependent upon the conditions of scrape-off plasmas. Those conditions have been discussed in the constraints for plasma edge and scrape-off conditions already.

Most of charged particles from the main plasma are assumed to flow into the divertor region without interacting with a first wall. However, when an RF option is adopted as a heating and/or current drive option, the scrape-off plasma with a certain densities is required in front of an RF launcher to assure a good coupling, and a some part of scrape-off plasma will interact substantially with the RF launcher and the first wall in the vicinity of it. E.g., a LH wave requires plasma density, (a few)$\times 10^{17} m^{-3}$ just in front of its launcher. Considering that temperature decays more rapidly than density, the plasma temperature is expected to drop to a rather low level at the top of the launcher, and consequently the impurity release and erosion problem could be eased. However, re-entering neutral particle from the launcher and its nearby first wall may provide an another problem, i.e., those neutrals could produce charge exchange neutrals with higher temperature, which will hit the first wall and sputter wall material. Such a problem has not been studied yet.

As the peak temperature and the peak particle flux at the divertor target are specified in the constraint for plasma edge and scrape-off conditions, the peak release rate of impurities from the divertor target and the peak erosion rate of the divertor target by D/T ions and He ions can be predicted as follows; 1.7×10^{19}atoms/m^2s and 2.6×10^{-10}m/s for tungsten target, and 3.6×10^{21}atoms/m^2s and 4.0×10^{-8}m/s for carbon target, where redeposition is neglected. When the sputtering by carbon and oxygen is taken into account, the peak release and erosion rates for the tungsten may be enhanced by a factor of around 5, which is however uncertain due to ambiguity of the sputtering yield. For the carbon target, in addition to the physical sputtering, the chemical sputtering further increase the release and erosion rates, e.g., by a factor of 2.

The predicted peak sputtering rate and peak erosion rate of the first wall near the divertor target due to charge exchange neutrals can also be evaluated from the maximum flux and its temperature mentioned previously and they are; 1×10^{22}atoms/m^2s and 3.2×10^{-10}m/s for stainless steel, and 1×10^{22}atoms/m^2s and 1.2×10^{-9}m/s for carbon, here redeposition is also neglected.

During a startup stage, the limiter option is included as a

potential candidate, in addition to the divertor option, as mentioned previously. The plasma temperature and density at separatrix, evaluated for the current rampup stage, are estimated as 1.4keV and $1.9\times10^{19}m^{-3}$. The peak release and erosion rates for D, T and He are 8.7×10^{-3}atoms/s and 4.9×10^{-11}m/s for carbon limiters, which do not cover uniformly in toroidal and poloidal directions, because of occasional independent maintenance.

CP 9 Plasma edge and scrape-off conditions

[Guideline for FER]

The most significant plasma parameters for single-null configuration are as follows.

(1) The plasma density and temperature in the outboard scrape-off layer on the midplane are assumed as follows,

(Plasma density)

$n(x) = n_s \exp(-x/\lambda_n) + n_b$

n_s = (a few)$\times 10^{19}$ m^{-3}

n_b = (a few)$\times 10^{18}$ m^{-3}

λ_n = (2-4)cm

(Plasma temperature)

$T(x) = T_s \exp(-x/\lambda_T) + T_b$

T_s = (100-200)eV

T_b = (5-10)eV

λ_T = (2-4)cm

(x is the distance from the separatrix)

The plasma density and temperature at different location should be estimated under the assumption that plasma parameters are almost constant on the identical magnetic surface around the main plasma.

(2) The predicted conditions at the divertor target are as follows,

-- Peak electron and ion temperatures are 20eV.

-- The density profile in front of the divertor target takes a form of $0.9\exp(-(x/\lambda)^2) + 0.1$. The total particle flux is 2×10^{24}/s for each target. The decay length, λ, is 8 and 4cm at the outboard divertor and 12 and 4cm at the inboard divertor, where the longer length is assigned to the region which connects to the scrape-off layer around the main plasma.

(3) The distance from the null-point to the divertor target along the separatrix line should be longer than 70cm. And the minimum distance from the null-point to the divertor plate should be larger than 10cm.

(4) Plasma conditions during startup can differ significantly from those during a burning stage. They also depend on an operation scenario. Details are not specified at present.

[Remarks]

Most of plasma edge and scrape-off conditions can be predicted by numerical results obtained from a divertor code, which analizes the scrape-off plasma around a main plasma and in a divertor region. The available divertor code coupled with neutral particles, which is still under development, is not in a satisfactory state, and the region to be covered is limited only within the divertor room at present, although a more simplified version can analyze the divertor and main plasmas altogether in a quite crude way. The divertor code also has not yet been developed to a level where it can handle impurity behaviours. The guideline mentioned above therefore is still preliminary.

According to the results from the divertor code, the localized recycling will cool the local plasma in the divertor room. The temperature and density in front of the divertor target will be reduced and enhanced, respectively, at least during the burning stage. Such observations are strongly influenced by conditions in the scrape-off layer external to the divertor, and the startup stage might have different conditions.

Reflecting such a less-developed state of the divertor analysis code, the parameters of the scrape-off plasma surrounding the main plasma are given as a guideline in a rather direct way, instead of giving coefficients of the cross field transport for heat and particle. The temperature and density at the separatrix are also given in a less-rigid way having certain ranges, because of ambiguities in the prediction. Based on latest simulation results of DIII experiments, in which the newly developed divertor code, covering the whole scrape-off layer, has been applied, the coefficients of the cross field transport for heat and particle, $\chi_{\perp}^{e} = 0.7 m^2/s$ $(2D^{Bohm})$ and $\chi_{\perp}/D_{\perp} = 4$ can well reproduce the temperatures and densities measured in the scrape-off layer. The decay length for temperature is also expected to become shorter than that for density.

The predicted conditions at the divertor target in the above guideline have also some ambiguities, because of the rather simplified divertor geometry for analyses, approximated by a rectangular shape, not a real divertor target inclining to magnetic fields. The peak electron and ion temperatures at the target may decrease less than 20eV, unless the inclination of the divertor target has substantial effects. The profiles of density and temperature at target may be strongly influenced by conditions exterior to the divertor, which are practically determined by the transport in the scrape-off layer around the main plasma. Since the present divertor code available for analyses does not reflect precisely such a situation, the above conditions at the divertor target have still uncertainties, and further studies are required. The following conditions are a typical example used in a design study; angle of target inclination, 20°, peak power load, $2MW/m^2$, width at half height for power profile, 7cm, peak electron temperature, 20eV, peak ion temperature, 20eV, peak plasma density, $2x10^{20}m^{-3}$.

During a startup stage, a plasma current is mainly ramped up non-inductively, while an inductive rampup will be utilized both at current initiation up to around 1MA and at the end of startup stage (ignition approach). It is quite desirable and beneficial that the high-recycling and low-temperature divertor concept is workable even during the startup stage. Since the plasma density may be reduced to around $1x10^{19}m^{-3}$ for efficient rampup, such a favourable divertor operation is uncertain while such a possibility is still being investigated. A limiter option therefore is included as a potential candidate, in addition to the divertor option. The plasma temperature and density at separatrix are evaluated for the current rampup stage in a conventional and crude way, and they are estimated as 1.4keV and $1x10^{19}m^{-3}$ for the limiter case, and 50eV and $1x10^{19}m^{-3}$ for the divertor case, when a 20MW power is applied for current drive.

CP11 Disruption scenario

[Guideline for FER]

The disruption scenario for FER is summarized as follows. The whole process can be divided into three stages. The first stage is for a period in which some instabilities are growing, but no changes can be observed externally. In the second stage, a part of plasma energy is rapidly released to the divertor target and plasma current profile becomes more broad, and negative voltage spike appears. At the third stage, for major disruptions, plasmas continue to release their energy with moving inwards and decreasing plasma current. A part of the magnetic energy of plasma current, which is stored in the space surrounded by the first wall, is converted into plasma thermal energy, and the other part is consumed in torus structures. In minor disruptions, on the other hand, plasmas can be restored to the original state, probably by the aid of heating power added externally.

Details are listed in the Table.

Table for disruption scenario

Scenario for major disruptions

(1) 1st stage

* Superficially, there is no change in plasma thermal energy and plasma current, while instabilities are growing internally.

(2) 2nd stage

* A part of plasma thermal energy is released rapidly with keeping plasma current constant.

* Plasma thermal energy decays with a time scale of 5ms (0.2ms). The longer time scale is a reference option and the shorter one in the parenthesis, which reflects latest experimental evidences, seems to have large impact on design. Such an impact will be studied locally, not in a consistent way withother structures.

* 40% of plasma thermal energy is released during this stage to the divertor target with the same profile of power flux as during burn.

* Negative spike voltage should be estimated from the following formula assuming change of plasma current;

$$\delta I_p = \dot{I}_{ns}\left(t - \frac{\tau_{ns}}{2\pi}\sin\frac{2\pi}{\tau_{ns}}t\right)$$

$\dot{I}_{ns}$ = 200MA/s (for major disruption)

$\dot{I}_{ns}$ = 20MA/s (for minor disruption)

τ_{ns} : thermal quench time

(3) 3rd stage

* Plasma current decreases, and the remainder of plasma thermal energy and a part of plasma magnetic energy continue to decay.

* Both of plasma current and plasma energy decay linearly with a time scale of 15ms (50ms). The shorter time scale is a reference one and the longer one in the parenthesis, which reflects possibility of controlling disruptions, may give a favourable impact on design, which will be elucidated.

* The sum of the remainder 60% of plasma thermal energy and plasma magnetic energy stored in the space surrounded with the first wall is dissipated on the first wall. The half of it is transfered onto the first wall at the inboard, occupying 30% of the whole first wall area, with a peaking factor of 2. The other half is deposited uniformly on the whole area of the first wall in the form of radiation.

[Remarks]

Plasma disruptions will heavily impact on the lifetime of plasma facing components to which the energy is discharged. The damage to be expected depends on energy density and decay time. Therefore, an analysis of the decay times, the energy involved and the surface area and location to which discharges are going, is very impotant. In spite of such importance, details of the disruption

scenario, especially, where and how the plasma energy is discharged, are still unclear and difficult to be specified, because of scarce detailed measurements due to their inherent difficulties. The above values considered for FER therefore do not follow precisely the specific experimental data. They reflect general judgements in the light of experimental observations and considerations in INTOR Workshop.

The above guideline is presented in a rather general way, therefore it is not appropriate to compare them with other disruption scenarios. The below table is prepared for such a purpose for a typical FER design.

As far as minor disruptions are concerned, their impacts on plasma facing components do not seem more severe than those of major disruptions. The scenario for the minor disruptions therefore has not been specified.

Table Main features of major disruptions

Frequency	
Stage I and II (6000shots)	5% (300)
Stage III (12000shots)	1% (120)
Total energy deposited per disrution	
Divertor plate[a]	58MJ
Uniform to the first wall[b]	87MJ
Local to the first wall[c]	87MJ
Peak energy flux	
Divertor plate	245J/cm^2
First wall	209J/cm^2

a/ Same distribution as operating load

b/ Radiation

c/ On 30% of first wall with an additional peaking factor of two

CP12 Particle exhaust and fuelling requirements

[Guideline for FER]

The following conditions should be satisfied;

(1) In order to maintain steady state burn conditions it is necessary to exhaust helium ash at the rate of α-particle production, i.e., 1.4×10^{20}/s.

(2) The necessary pumping speed may depend on to what extent neutral gas is compressed in the divertor region. Studies on high recycling divertor can provide some information on the pumping requirement and the pumping speed is selected to be 1×10^{5} l/s at the entrance of pumping ducts.

(3) The typical concentration of evacuated gas through pumping duct is assumed to be almost same as that of a main plasma; 46% for deuterium and for tritium, 5% for helium, 0.5% for carbon, 0.5% for oxygen, 1% for hydrogen and less than 0.1% for nitrogen.

(4) The fuelling method is hybrid use of gas puffing and pellet.

[Remarks]

The conditions for particle exhaust are evaluated on the basis of the divertor studies, in which an analyzed region is somewhat expanded as including a part of exhausting duct, although the divertor geometry is still simplified to a rectangular one. The powerful localized recycling and the accompanying buildup of neutral pressure near the divertor target depend not only on the conditions of scrape-off layer exterior to the divertor region as mentioned previously, but also on the divertor geometry. Such favourable features of powerful recycling can be easily realized for the closed-type divertor, which is featured by the rather long divertor throat and the relatively narrow gap between plasma boundary and first wall. Inversely, the open-type divertor geometry, featured by the short divertor length and the wide distance for plasma-boundary-to-first-wall, is difficult to produce localized high recycling divertor plasma and resultant strong buildup of neutral pressure. Careful attentions should be paid on the divertor geometry to get beneficial divertor performance.

Given the rather closed-type divertor configuration, the

pumping requirement is quite easy, e.g. in a certain favourable condition, pumping speed less than $1x10^4$ l/s, which is needed at entrance of pumping duct, is adequate for removing the specified helium ash. The total pumping requirement $1x10^5$ l/s is selected, considering ambiguities in the incoming particle flux to divertor, in the modelling and the practical divertor configuration.

Particle species handled in the present divertor code are limited to deuterium, tritium and helium. The helium enrichment/de-enrichment are strongly model-dependent in numerical calculations. In DIII, the slight de-enrichment of helium was observed, although the experimental condition was not the same as that of the DT burning plasma. Thus, there is no definite evidence that the concentration of exhausted gas differs from that of a main plasma. The ingredient of the divertor plamsa is then assumed to have the same one as the main plasma. The enhanced flow of D/T and helium ions to the divertor target are assumed as; $1x10^{24}$/s for each (inner and outer) target, and $1.1x10^{23}$/s for helium ions.

It is also necessary to supply fuel D/T neutrals. The fuelling method is the hybrid use of gas puffing and pellet, which are usual supply methods in the present-day tokamaks. The gas will be puffed into the divertor room, partly because it might aid the hugh recycling mechanism, and partly because the gas puffing into the main plasma may be against the so-called H-mode trend and it may also produce high energy charge exchange neutrals which could interact the first wall. The penetration of pellet to a plasma center may need its speed more than 10km/s, which may require elaborate development effort for the next step device. Considering uncertainties in particle transport physics, suggesting an anormalous inward flow, the pellet speed of a few km/s is appropriate and realistic for FER pellets. Thus the emphasis of the pellet is placed on the initial density build-up phase.

CP13 Power deposition efficiency and profile

[Guideline for FER]

It may be an useful information for plasma heating system design to get what part of launched power is deposited into a plasma, i.e., $\eta_{dep}^{Global} = P_{dep}/P_{inj}$. It depends strongly upon plasma parameters and characteristics of heating methods. Details have not been specified till now.

The profile of deposition power can also be specified, when details of a heating method and profiles of plasma parameters are fixed. It is, however, difficult to specify it in a general way.

The strong constraint for favourable deposition profile foe heating power does not seem to exist, when an extreme profile, such as surface heating, is avoided. In addition, if the profile consistency really governs the plasma transport process, difference of the heating profile little affect the plasma performance as long as the dominant part of the heating power deposits within the confinement region, possibly q=2 surface.

CP14 Current drive efficiency and profile

[Guideline for FER]

The normalized current drive efficiency, defined as $\gamma = \bar{n}_e[10^{20}m^{-3}]I_0[MA]R_0[m]/P_{inj}[MW]$, is different for each drive method.

(Lower hybrid wave)

The normalized current drive efficiency γ, given as

$$\gamma = 0.1 - 0.3,$$

is used for FER, based on JT-60 LHCD experiments. The current rampup efficiency, defined by $\gamma_{ramp}=P_{el}/P_{inj}$ (P_{el}: increasing rate of the stored magnetic energy of the plasma), is

$$\gamma_{ramp} \sim 0.1 - 0.2,$$

which has been also observed in JT-60 current ramp-up and recharging experiments.

(Neutral beam)

The normalized current drive efficiency depends on many parameters, such as plasma density and temperature, their profiles, plasma purity, and beam energy and its spacial distribution. The following efficiencies are typical ones obtained through rather sophisticated procedures.

γ =0.353 (By means of an orbit following Monte Carlo code under a condition with $\bar{T}_e$=20keV, $\bar{n}_e=0.7\times10^{20}m^{-3}$, Z_{eff}=2.2, E_b=0.5MeV),

γ =0.32 (Through an analytical solution of Fokker-Planck equation under the same condition as the above except for Z_{eff}=1.8).

(Fast wave)

The current drive efficiency should follow the expression given by Fisch-Boozer.

$$\gamma \lesssim 1.5\times10^{-6}\,\bar{T}_e\,\frac{20}{\ln\Lambda}\,\frac{8}{5+Z_{eff}}\,w^2 = \frac{6.3}{Z_{eff}+5}\,\frac{20}{\ln\Lambda}\,\frac{1}{n_{//}^2},$$

$$w=v_{//}/v_t, \qquad \bar{T}_e[eV].$$

This value gives the upper limit imposed by the theory for both low and high frequency fast wave.

(Current profile)

The profile of the total current consisting of non-inductively driven current, Pfirsh-Schluter current and bootstrap current must be consistent with MHD stable one. The non-inductive current drive method therefore should have capability providing a wide variety of profiles from peaked to hollow ones. The combination of those various profiles can provide a current profile approximately desirable to MHD stable ones, e.g., preparing RF waves with several kinds of frequencies, or several neutral beams with changeable energy and beam lines going through different points in a plasma.

[Remarks]

(Lower hybrid wave)

Recent JT-60 LHCD experiments demonstrate that LHCD is a promising candidate for non-inductive current drive of the reactor relevant plasma. In the experiments, the maximum plasma current 1.7MA with RF power P_{inj}=1.2MW at f=2GHz are successfully obtained [1].

High current drive efficiency γ=0.1-0.17 is obtained even in the relatively low temperature regime ($T_e \simeq$ 1-2keV). When NBI heating is combined with LHCD, γ drastically increased to $\gamma \simeq$ 0.2-0.3. The temperature dependence of the current drive efficiency is shown in Fig. 1 [2], which implies that the driving efficiency could be further enhanced with increasing the temperature. Experimental data bases from small- and medium-size tokamaks are also shown in Fig. 1.

Current rampup and transformer recharging experiments were also carried out in JT-60 and $\gamma_{ramp} \simeq 0.2$ has been obtained with rough estimation [2].

An useful expression for simple estimation of average rampup efficiency $\bar{\gamma}_{ramp}$ can be obtained using the analytical solution for the 1D Fokker-Planck equation and plasma circuit equation [3]. The expression is

$$\bar{\gamma}_{ramp} = \frac{\int_0^{t_{ramp}} P_{el}\,dt}{\int_0^{t_{ramp}} P_{in}\,dt} = \frac{2}{Kb\theta} P_{el}\,, \qquad (1)$$

$$P_{el} = g(x_1) - g(x_0),$$

$$g(x) = \frac{x^2}{2} - 2x + (2-b)\ln(x+1) - \frac{b}{x+1}\,,$$

$$x_0 = (1+b)^{1/2}, \quad x_1 = (1+b^{-\theta})^{1/2}\,,$$

$$b = 5.179\times10^{4}\,(n_{z2}^{-2} - n_{z1}^{-2})\exp(-c/n_{z1}^{2}T_e)\,\frac{\ln(n_{z1}/n_{z2})}{T_e^{2}}\,,$$

$$\theta = t_{ramp}/\tau, \quad \tau = L_p/R_p,$$

K : numerical factor (0.392).

Note that Eq.(1) is valid under the condition that the inductive field $E_{//}$ does not become large ($E_{//}/E_{DC} \ll 1$, E_{DC} is Dreicer field), and the effect of runaway electron can be neglected. A numerical code is used to evaluate the efficiency and check the estimation from Eq.(1). The code follows time evolution of the plasma power balance and circuit equation. The analytical solution of 1D Fokker-Planck equation is used to calculate the absorved RF-power and the driven current in the code. Karney and Fisch [4] have included the effect of runaway elecrtros by numerically solving the 2D Fokker-Planck equation. They also obtained the simple estimation formula,

$$\gamma_{ramp} = \frac{1}{u}\frac{\partial w_s}{\partial u} \sim \frac{\sum_{i=1}^{3} a_i u^{2i}}{\sum_{i=0}^{3} b_i u^{2i}}\,, \qquad (2)$$

$$u = v/v_r,$$

$$v_r = \left(\frac{m_e \Gamma}{|qE_{//}|}\right)^{1/2}, \quad \Gamma = \frac{n_e q^4 \ln\Lambda}{4\pi\varepsilon_0^2 m_e^2},$$

which is valid for $u \sim u_{//}$ and $0 < u < 5$ by numerical fitting for the solution of the 2D Fokker-Planck equation. Both Eqs.(1) and (2) give rampup efficiency γ_{ramp} of about $0.1 \sim 0.2$ for the condition that $n_e = 0.7\times10^{19}\,m^{-3}$, rampup time $t_{ramp} = 200s$, $L_p = 10\,\mu H$, $I_p = 8MA$, $n_{//} = 2$, $Z_{eff} = 2$, and $u_{//} = 0.7$. Using this value for γ_{ramp}, the required power P_{inj} can be estimated by

$$P_{inj} \sim \frac{\frac{1}{2}LI^2}{\eta_{ab}} \eta_{ramp}^{-1} , \qquad (3)$$

where η_{ab} is the ratio of absorbed power P_{ab} to injected power P_{inj}. From Eq.(3), $P_{inj} \sim$ 10-20MW may be required for the above rampup condition.

References

[1] T. Imai, et al., 11th Int. Conf. Plasma Phys. Contr. Nucl. Fus. Res., IAEA-CN-47/K-I-2(Kyoto) 1986.

[2] K. Sakamoto, et al., JAERI-M 87-061(1987).

[3] T. Okazaki, et al., Nucl. Fusion 26(1986) 1029.

[4] C.F.F. Karney, et al., Phys. Fluids 29(1986) 180.

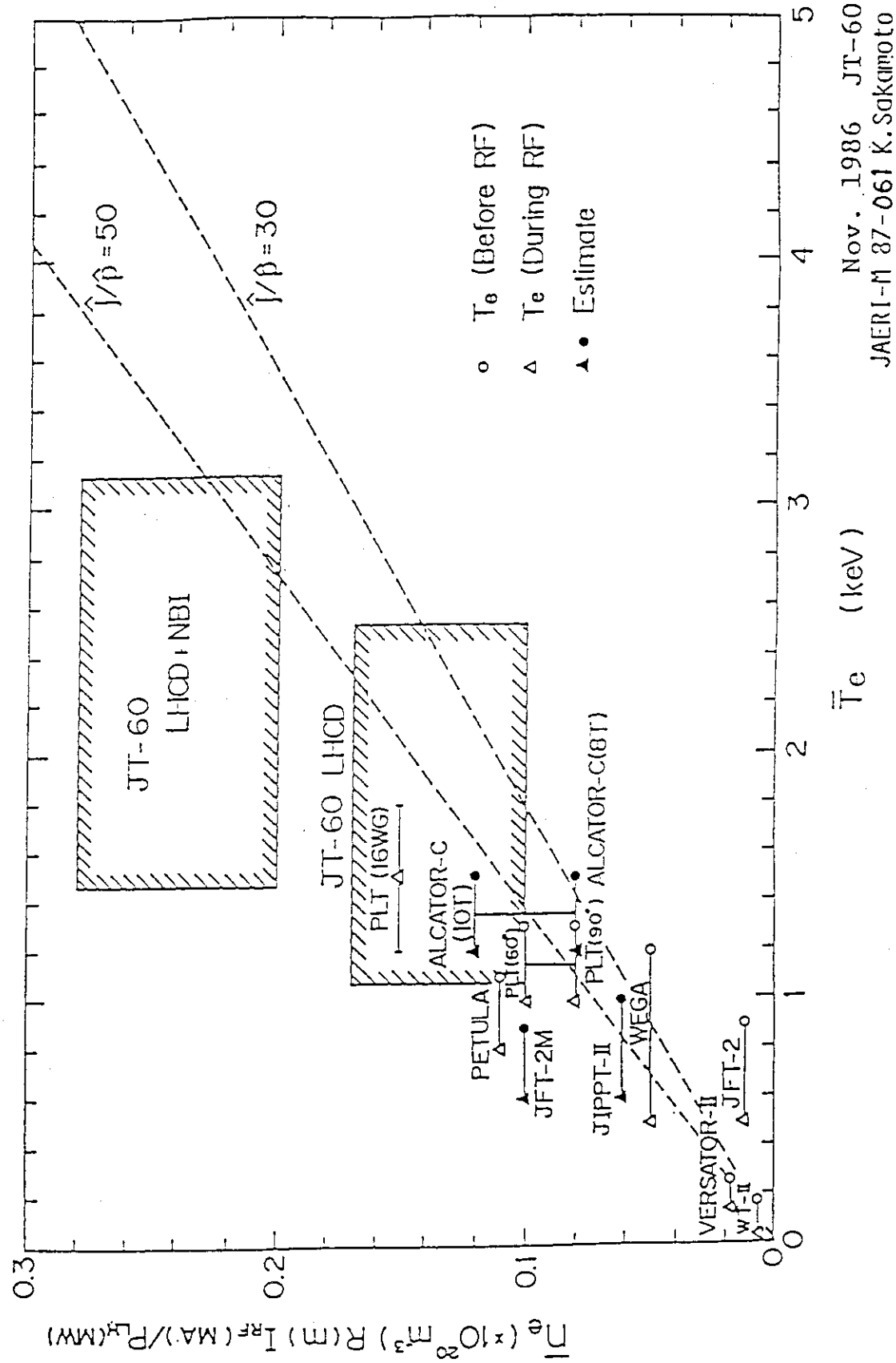
Fig.1 Current Drive Efficiency
$\hat{I}/\hat{P}=50$
$\hat{I}/\hat{P}=30$
JT-60 LHCD+NBI
JT-60 LHCD
PLT (16WG)
ALCATOR-C (10T)
PETULA
PLT(16G)
JFT-2M
PLT(90°)
ALCATOR-C(8T)
JIPPT-II
WEGA
VERSATOR-II
JFT-2
o Te (Before RF)
Δ Te (During RF)
▲● Estimate
Nov. 1986 JT-60
JAERI-M 87-061 K.Sakamoto et al.
$\bar{T}e$ (keV)
Π_e ($\times 10^{20}$ m^{-3}) R(m) I_{RF}(MA)/P_{LH}(MW)

(Neutral Beam)

Two different analysis codes are used to evaluate the current drive efficiency. The one is an Orbit Following Monte-Carlo (OFMC) code, which calculates beam deposition and subsequent collisional evolution of the fast ion trajectories in an axisymmetric tokamak with elliptical cross section. The OFMC code is coupled with a transport code, an equilibrium code and a ballooning stability code. The current drive efficiency can be obtained at an arbitrary level of consistency, e.g., the consistent solution with an equilibrium without stability consideration. The other one uses the analytical solution of 2D Fokker-Planck equation with a non-circular geometry, also coupled with an equilibrium code and a power balance code. The latter code is able to make small adjustments and is used for parametric studies.

The current drive efficiency in the above guideline is from the consistent solution, satisfying power balance and plasma equilibrium, without the stability consideration. The current drive efficiency depends upon plasma and beam parameters, such as plasma density and temperature, effective ionic charge, and beam energy, and may furthermore upon plasma profiles and size, and beam geometry. The general expression for the current drive efficiency is therefore difficult and then some parametric studies are summarized in the followings.

The drive efficiencies are evaluated for an INTOR-like device with R_0=4.9m, a=1.17m, κ=1.5, ε=0.3, parabolic profiles for density, temperature, and current, I_0=8MA. With the adoption of multi-beamlines, each neutral beam power is automatically adjusted to give the parabolic current profile. Table 1 shows currnt drive efficiency with differnt beam energy. In Fig. 1, the drive efficiency is depicted with the beam energy for two average densities. At the low density, the efficiency I_p/P_b is maximized at E_b=1MeV and for the beams with more than 1MeV it decreases due to the shinethrough, while the high density case has the peak at E_b=1.5MeV. The Z_{eff} dependence is quite weak, as shown in Fig. 2. The temperature dependence is rather strong, as seen in Fig. 3, where the beta value is fixed.

The profile control of driven current is very crucial for beta

enhancement, suppression of sawtooth oscillation, and avoid of plasma disruptions. The realistic method for plasma profile control was proposed at JAERI, using a negative-ion-based neutral beam injection system [1].

In the NBI system, almost all beams are not neutralized at the entrance of the neutralizer, because of low system pressure. Hence, by changing the beam power profiles with horizontal magnetic fields, less than 0.03T, produced by coils in the beam profile controller, the beam driven current profile is easily controlled. Figure 4 shows typical beam driven curent profiles J^{NBI} corresponding to three beam power profiles along a vertical direction at R_{tang}, which is the minimum major radius along the beam path. Global beam driven current efficiency $I_b[A]/P_b[W]$ and beam shine-through fraction f_s are also shown. Figure 4 shows only capability of current profile control, because target plasma parameters are fixed. The upper and lower beam profiles with respect to the equatorial plane can be controlled independently. Required total beam driven current and its desirable profile, depending on scenarios, can be obtained by the combination of individual current profiles obtained in a few units of the NBI system [2].

References

[1] S. Yamamoto, et al., in Plasma Physicss and Controlled Nuclear Fusion Research, (11th Int. Conf. Kyoto, 1986) Paper IAEA-CN-47/H-I-3.

[2] Y. Okumura, et al., Proc. of 11th Symp. on Fusion Engineering, Austin, 1985.

E_b/MeV	$\gamma = I_0 R_0 n_e / P_b$
0.5	0.32
1.0	0.35
1.5	0.32
2.0	0.29

Table 1 $\overline{n_e} = 0.7\times10^{20}m^{-3}$, T_e = 20 keV.

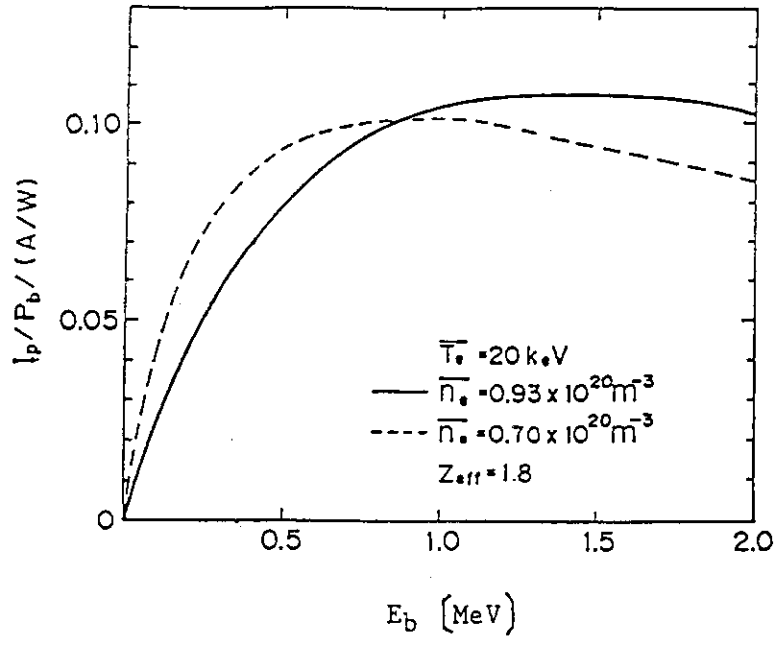

Fig. 1 E_b dependence of I_p/P_b

----- : $Te = T_0(1-x^2)$, $n_e = n_0(1-x^2)$, $\overline{n}_e = 0.70\times10^{20}m^{-3}$.

——— : $T_e = T_0(1-x^2)$, $n_e = n_0(1-x^2)^{0.3}$, $\overline{n}_e = 0.93\times10^{20}m^{-3}$.

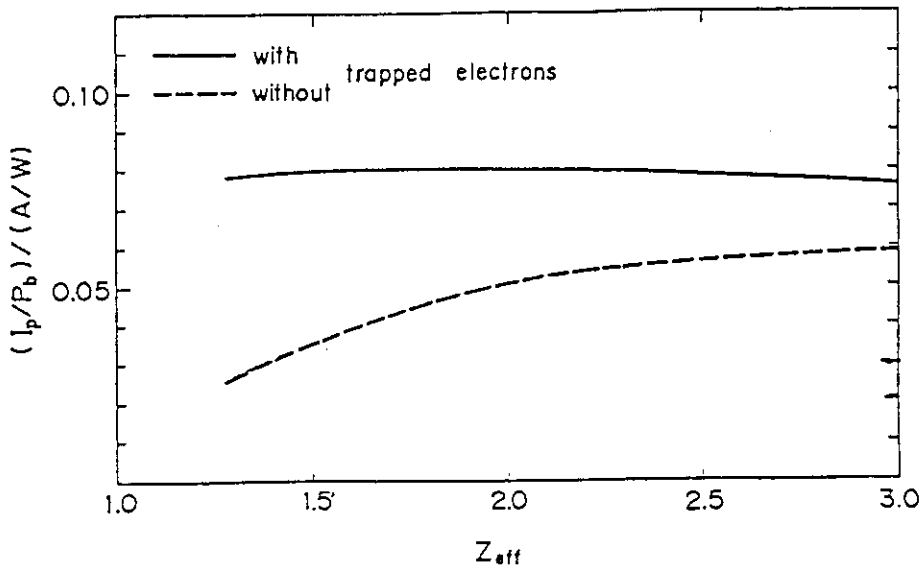

Fig. 2 Z_{eff} dependence of I_p/P_b

$\overline{T}_e$ = 20 keV, $\overline{n}_e = 0.93\times10^{20}m^{-3}$, E_b = 0.5 MeV.

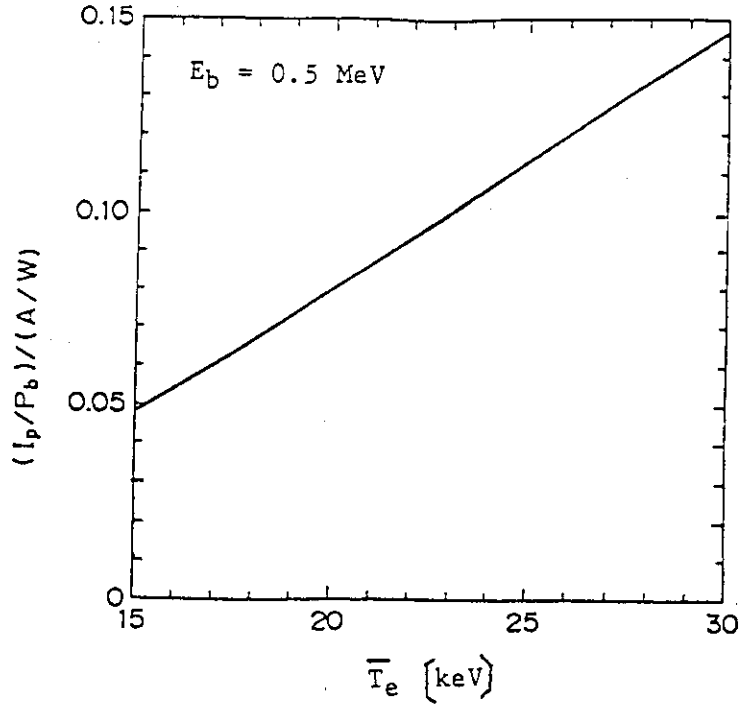

Fig. 3 $\overline{Te}$ dependence of I_p/P_b

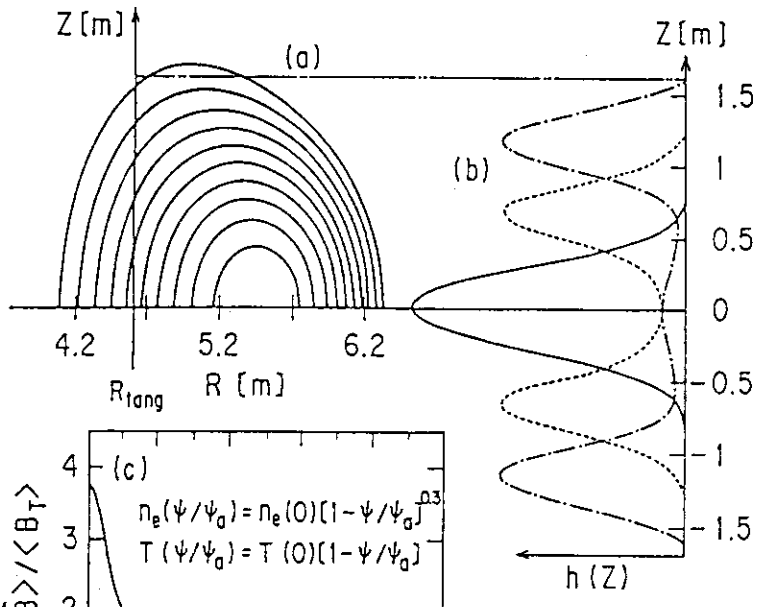

Device parameter

$E_b = 500\,keV$, $R_{tang} = 4.6\,m$

$B_T = 5.3\,T$

Plasma parameters

$R_0 = 5.2\,m$, $a = 1.12\,m$

$\kappa = 1.5$, $Z_{eff} = 2.2$

$\bar{n}_e = 0.7 \times 10^{20}\,m^{-3}$

$\bar{T}_e = \bar{T}_i = 20\,keV$

(d)

	———	·····	—·—·—
$I_b[A]/P_b[W]$	0.097	0.10	0.10
$f_s\,(10^{-2})$	~ 0	~ 0.3	~ 2

Fig. 4

(Fast wave)

The current drive efficiency can be smaller than that of LH wave due to discrete spectrum of fast wave, when both methods use Landau damping as the current drive mechanism.

CP15 Parameter ranges for heating and current drive

[Guideline for FER]

There are a lot of constraints and they depend upon a method involved. Constraints are therefore described separately.

(LH current drive)

(1) The maximum operating density is limited by "density limit" for LHCD. The critical density n_c for density limit is propotional to square of the wave frequency, i.e., $n_c \propto f^2$.

(2) Lower operating density is preferable for efficient current drive. However, very low density ($< 10^{19} m^{-3}$) plasma may be difficult to be produced reliably in large devices.

(3) For current rampup, the lower temperature is preferable for shortening the current rampup time, which is required from the duty cycle requirement. The higher temperature, on the other hand, is favourable for steady state operation.

(4) The frequency should be higher than the switch-over frequency, f_{sw}.

$$f_{sw}^2 = \frac{n_e}{2.28}\left(\alpha + \frac{\Sigma^2}{Z_0^2}\sum_i \frac{T_i}{A_i T_e}\right) - \frac{1.03}{B_T^2}$$

(5) Parametric instability should be avoided, i.e.,

$$f \gtrsim 2 f_{LH}(0)$$

$f_{LH}(0)$: LH frequency at plasma center

(6) The refractive index should be large enough to avoid mode conversion to fast wave;

$$N_{//} > N_{// AC}$$

$$N_{// AC}^2 = 1 + f_{pe}^2 / f_{ce}^2 \Big|_{r=0}$$

(7) Mode conversion to an ion plasma wave should be also avoided;

$$N_{//} < N_{// MC}$$

$$N_{// MC} = \left(\frac{f^2}{f_{LH}^2} - 1\right)\left[2\sqrt{3}\frac{v_{eth}}{c}\left(\frac{T_e}{T_i}\right)^{1/2}\left(1+\frac{T_e}{T_i}\hat{f}^4\right)^{1/2}\right]^{-1}$$

$$\hat{f}^2 = f^2/(f_{ce} f_{pe})$$

(8) The low $N_{//}$ and narrow spectrum is preferable for efficient current drive considering experimental data.

(9) Transmission coefficient, (1-R) should be large, which constrains plasma edge density.

$$1-R = \exp[-2(x_p+L_n)/\lambda_x]$$

$$L_n[m] = 1.24\times10^{-2} f^2 (dn_e/dx)^{-1}$$

$$\lambda_x[m] = c/2\ f\sqrt{N_{//}^2-1}$$

E.g., $(1-R) \gtrsim 0.5$ needs $x_p+L_n \lesssim 0.5$cm for f=2GHz, and $N_{//}=2$.

(NB current drive)

(1) The plasma density should be large to avoid excessive shinethrough, which depends upon beam energy and spatial geometry, plasma parameters, and tolerable heat of armour plate for shinethrough. The minimum plasma density, therefore, cannot be simply specified.
E.g., plasma with $n_e=1\times10^{19}m^{-3}$ yields 20% shinethrough by NB with E_b=500keV. This shinethrough power is within the allowable limit of the armour, i.e., the average heat flux of $4MW/m^2$ with a peaking factor 1.5.

(2) The maximum beam energy is limited to 500keV, which is not the optimum one for NB current drive. The limit comes from a resonable span of development on negative ion based NB system.

(3) The condition that beam current equals to electon current should be avoided, which depends on Z_{eff}. The higher Z_{eff} is favourable for the curent drive efficiency.
For steady state operation, $Z_{eff}\sim2$ is preferable, taking into account reduction of fuel particles.
For rampup and recharging, $Z_{eff}\sim10$ may be favourable, considering reduction of time scale of startup and recharge.

(4) For steady state operation, the current drive efficiency is increased with higher temperature and lower density. However, the minimum density may exist in order to realize the high recycling divertor plasma and to avoid severe impurity contamination of plasma and large erosion of target, as mentioned in the previous LH current drive.

(5) In the rampup stage, the β-limit seems quite severe for NB current drive, because of additional pressure due to fast beam. Especially, during small current, poloidal beta limit may be a strong constraint, i.e.;

$$\beta_p \lesssim \frac{1}{2}A$$

(Fast wave current drive)

(1) The frequency range of low frequency fast wave should be

$$f > 1.5 f_{CD}.$$

The frequency range of high frequency fast wave should be

$$f = (10\text{-}20) f_{CD} < f_{LH}.$$

(2) The density of scrape-off layer in front of antenna should satisfy

$$n_s > 3\times10^{17} m^{-3}.$$

(3) The electric field polarization should be in the poloidal direction, and a toroidal component should be suppressed by Faraday shield.

(IC heating)

2nd harmonic for deuterium is selected for IC heating.

(1) The frequency should be $2f_{CD}$,

$$f_{CD}[\mathrm{MHz}] \simeq 7.6 B_T[\mathrm{T}].$$

(2) The density of scrape-off layer in front of launcher should meet

$$n_s \gtrsim 3\times10^{17} m^{-3}$$

to get good coupling.

(3) The launched wave spectrum should satisfy

$$k_{//} > \omega/c$$

to avoid coaxial mode.

(4) Damping by α-particles cannot be avoided, since the following damping condition is satisfied

$$k_{//} > 0.5a/R.$$

Thus, heated α-particles must be well confined under a condition of

$$I_p[\mathrm{MA}] \gg 5.4(a/R)^{\frac{1}{2}}.$$

(LH heating)

For electron heating

(1) The frequency must meet

$$f \gtrsim f_{sw} \quad \text{(see LH current drive)}$$

$$f \gtrsim 2f_{LH}(0) \quad \text{(see also LH current drive).}$$

(2) The wave spectrum should satisfy

$$N_{//AC} < N_{//} < N_{//MC} \quad \text{(see LH current drive),}$$

$$N_{//} \gtrsim (5\text{-}7)/T_e^{\frac{1}{2}}[\text{keV}].$$

(3) For coupling, almost same as LH current drive.

For ion heating,

(1) The frequency must meet

$$f_{sw} \gtrsim f,$$

$$f \sim f_{LH}(0).$$

(2) The wave spectrum should satisfy

$$N_{//} \gtrsim N_{//MC},$$

$$c/N_{\perp} v_{ith} \lesssim 3.0\text{-}3.5.$$

(3) For coupling, almost same as LH current drive.

(NB heating)

(1) The beam energy of more than 250keV is required for tangential injection to heat INTOR-like plasmas.

(2) For shinethrough, almost same as NB current drive.

(Electron cyclotron heating)

Fundamental ordinary wave (O-mode) is chosen for electron cyclotron heating method to assist pre-ionization and pre-heating.

(1) The frequency should be set

$$f = f_{ce}(0).$$

(2) To avoid the cutoff, the frequency should be

$$f > f_{pe}(0).$$

(3) Antenna should be installed in the low-field side of the torus.

(4) Single pass absorption rate may be unity for temperatures

higher than 1keV. Heating efficiency has the range of $(2\text{-}7)\times10^{19}m^{-3}eV/kW$, which has been observed experimentally.

[Remarks]

(LH current drive) [1]

The following three characteristics are considered for physics design process for LHCD.

(1) Wave propagation in a plasma.

(2) Efficient power absorption within a plasma (to minimize the required power).

(3) Efficient coupling characteristics between RF launcher and plasma.

These characteristics depend mainly on the choice of the following parameters,

(1) target plasma condition for LHCD

-- target plasma density and temperature,

(2) wave frequency

-- f,

(3) wave spectrum

-- $N_{//0}$: refractive index at spectrum peak,

-- $\Delta N_{//}$: spectrum width.

The LH wave for the current drive has the critical density, beyond which no driven current can be observed. In the old FER design (FY'85 FER), the operating density for LH current rampup was selected to be rather small $\bar{n}_e=3\times10^{18}m^{-3}$ because of the density limit mentioned above and current drive efficiency. Wave frequency was chosen to be f=0.56GHz so as to satisfy the condition $f>2f_{LH}(0)$ to avoid the parametric decay instability.

On the other hand, higher frequency (f=2GHz) is chosen in the present (FY'86 FER) design, mainly because

(1) recent experimental observations suggest that the critical density n_c for LHCD can be raised by increasing the wave frequency ($n_c \propto f^2$) and thus operating density region will be widened by higher frequency choice,

(2) very low density plasma like $n_e \sim 3\times10^{18}m^{-3}$ may be difficult to be produced and maintained reliably for large tokamaks, such as FER and INTOR.

The current drive efficiency, however, decreases with increasing

densities. Considering the large current to be ramped up in a relatively short period, around 100s, the lower density may be favorable to reduce the RF power requirements. Optimization for the operating density and required power has not been done yet.

Another problem accompanied with higher frequency choice is anticipated as follows;

(3) coupling efficiency between plasma and launcher might be decreased, since the decay wave length $\lambda_\perp$ in the vacuum region is expressed as

$$\lambda_\perp = c/f(N_{//}^2-1)^{0.5}, \qquad (1)$$

where c is velocity of light,

(2) wave guide design becomes more difficult, because its width $b_p + d_p$ decreases with increasing f,

$$b_p + d_p = \frac{c}{f N_{//0}} \frac{\Delta\phi}{2\pi}. \qquad (2)$$

As can be seen from Eqs.(1) and (2), small $N_{//0}$ is favorable for coupling and wave guide design when f is large.

The "spectrum gap" problem is critical issue for the choice of the wave spectrum $(N_{//0}, \Delta N_{//})$. Recent JT-60 LHCD experiments suggest that small $N_{//0}$ wave can drive large current. Also, Fisch-Karney theory predicts that small $N_{//}$ is favorable for the fast plasma current rampup.

Based on these considerations, higher f (2GHz) and lower $N_{//0}$ (~ 2) with narrow width ($\Delta N_{//} \simeq 1$-2) has been chosen as a reference scenario in the present design.

References

[1] A. Hatayama, M. Sugihara, K. Okano et al., "Lower Hybrid Current Drive and Heating for FER", to appear in 14th European Conference on Controlled Fusion and Plasma Physics, Madrid(1987).

(IC heating)

(1) $f_{CD}[MHz] = Z_i eB_T/m_i = 7.6B_T[T]$ for deutrium.

(2) Launched wave frequency f must satisfy $f > f_{pi}$ in front of the launcher (Faradey shield) to avoid a strong surface damping due to hot wave modes, where f_{pi} is the ion plasma frequency given by

$$f_{pi} = (Z_i^2 n_i e^2/m_i \epsilon_0)^{1/2}/2 \quad .$$

With f=80MHz, $f > f_{pi}$ gives $n_i > 3\times10^{17} m^{-3}$.

(3) In order to minimize an impurity generation by a coaxial RF mode, the wave power radiated in the regime $k_{//} < \omega/c$ must be minimized as low as possible.

(4) Resonance condition of alpha particles is

$$f_{min} < f - k_{//} v_{//\alpha}/2\pi < f_{max} \ ,$$

$$f_{min,\ max} = Z_\alpha eB_T(R=R_0+a,\ R_0-a)/2\pi m_\alpha \ .$$

Usually, this condition is satisfied for all alpha particles. Therefore the RF damping due to the alpha cannot be avoided. The condition inhibiting alpha particle orbit loss is

$$I_p[MA] \gg 5.4(a/R)^{1/2} \ .$$

DP16 Plasma heating power flow

The heating power of a main plasma, the sum of α-heating power and powers externally added, is consumed in various forms. Some power is radiated onto the first wall, and some finally transported to the divertor target. The heat flow is assumed as follows.

(1) The sum of the α-heating and external powers is lost through the following three paths within the confinement region of a main plasma;
   -- 20MW is consumed through bremsstrahrung and cyclotron radiations,
   -- 10% of the α-heating power is directly lost mainly due to toroidal field ripple,
   -- The remainder power is transported to a plasma egde

(2) The transported power to the edge is divided into three forms and lost within the edge-plasma;
   -- 15MW is radiated by light impurities,
   -- 3MW is consumed through charge exchange,
   -- The remainder power goes to the divertor region.

(3) The power transported to the divertor is consumed through three processes in the divertor region;
   -- lost by charge exchange,
   -- lost by fuel and impurity radiations,
   -- transported to the divertor target through a sheath.
   (Several different scenarios have been prepared and not finalized yet.)

(4) Heat flow distributions for startup and shutdown significantly differ from the above for the burning stage. Details have not been specified yet.

[Remarks]

How the plasma heating power is consumed and how the power is discharged on the first wall and the divertor target are of impotance for designing components facing plasmas. A transport code for a main plasma coupled with a scrape-off region, with an aid of a divertor code, is to provide most of answers to those questions.

The transport physics, governing numerical codes, however, is still quite uncertain and the codes are also under development. In this sense, the above guideline is still preliminary.

Most of fast α-particles, born in a relatively high temperature plasma region, are assumed to slow down within the almost same region, although the analysis with an orbit-following Monte-Carlo method suggests that the α-heating power deposition profile becomes rather broad. A part of fast α-particles escapes from a plasma mainly due to a toroidal field ripple. The power loss related to those effects are evaluated with an orbit-following Monte-Carlo method, the result of which is not trivial and has been already discussed in the toroidal field ripple. The loss power radiated through bremsstrahrung and cyclotron is dependent on plasma conditions, and the guideline of 20MW together is an averaged value, based on a lot of numerical results. The direct α-particle loss is so significantly localized that the design of first wall might be influenced greatly. On the othewr hand, the power of bremsstrahrung and cyclotron is radiated uniformly.

A part of the power transported to the plasma edge is radiated by light impurities, carbon and oxygen ions. A part of the power is also consumed by charge exchange neutrals, which will be localized near the divertor, in which the powerful particle recycling is working. When an RF launcher, requiring a plasma with a certain density near it, is installed, weak plasma-wall interaction will cause the power loss, including charge exchange loss. That interaction seems to be of some significance, however it has not been estimated yet.

In the divertor region, the powerful particle recycling cools plasma temperature and enhances density near a divertor target. The divertor analysis code is a most useful tool, predicting how the power transported to the divertor is consumed and deposited. The present divertor code available is however still not in a satisfactory state, especially it can only handle the simplified divertor geometry and it can not treat impurities. Taking into account those situations, the guideline for the divertor is tentatively given as follows. Several scenarios have been prepared for the power flow within the divertor, from optimistic to

pessimistic. The optimistic scenario is that a significant part of the power is radiated before entering the divertor target. In the most pessimistic one, the power 15MW, assumed to be radiated in the plasma edge, is neglected and instead that power is added to the power transported to the divertor, and furthermore the excess power is directly transfered to the divertor target without any radiation loss. The typical power flow is shown in Table.

During a startup stage, a plasma current is ramped up mainly non-inductively. Based on present analyses available, it is quite quetionable that the high-recycling divertor operation is workable during the startup stage. A limiter option is proposed as a potential candidate, in addition to the divertor option. The power for the startup current drive is crudely assumed to go to the limiter or divertor, without losing its power.

Table Power flow of typical FER design

(1) In the confinement region of the main plasma,
- -- 81MW : α-heating power
- -- 20MW : bremsstrahrung and cyclotron radiation,
- -- 8MW : direct α-particle loss,
- -- 53MW : to the edge-plasma.

(2) In the edge-plasma,
- -- 15MW : impurity radiation,
- -- 3MW : charge exchange,
- -- 50MW* (35MW) : to the divertor region.

(3) In the divertor,
- -- the most pessimistic scenario is that 50MW is directly transfered to the divertor target without loss,
- -- in the optimistic case, the considerable part of the power is radiated in the divertor region.

*) This value is for the pessimistic case. The radiation by impurities in the edge is assumed to be neglected, considering uncertainty in impurity behaviours.

IV. Summary

The plasma design philosophies for the FY86 FER conceptual design are stated. They are classified into two groups, physics design drivers and physics design constraints, according to the feature whether or not a designer is free to choose his option. Twelve design drivers have been picked up and the choices for them are elucidated. Sixteen design constraints have also been evaluated and the guidelines for them are described.

Acknowledgements

The authers would like to express their appreciation to FER engineering design team members, especially Dr. H. Iida: a team leader, Dr. R. Saito: a group leader of a plant system group, Dr. T. Kobayashi : a leader of a reactor structure group, Dr. N. Miki: a group leader of a magnet group, and Dr. K. Nakashima: a group leader of a electrical group for their fruitful discussions.

The authors also would like to express their appreciation to Drs. S. Mori, K. Tomabechi, M. Yoshikawa, and S. Tamura for their continued support.